Sedimentary Geology 335 (2016) 51–65

Contents lists available at ScienceDirect

Sedimentary Geology

journal homepage: www.elsevier.com/locate/sedgeo

Detrital cave sediments record Late Quaternary hydrologic and climatic variability in northwestern Florida, USA

Tyler S. Winkler [a,b], Peter J. van Hengstum [a,b,*], Meghan C. Horgan [b], Jeffrey P. Donnelly [c], Joseph H. Reibenspies [d]

[a] Department of Oceanography, Texas A&M University, College Station, Texas 77842, USA
[b] Department of Marine Sciences, Texas A&M University at Galveston, Galveston, Texas 77554, USA
[c] Department of Geology and Geophysics, Woods Hole Oceanographic Institution, Woods Hole, Massachusetts 02543, USA
[d] Department of Chemistry, Texas A&M University, College Station, Texas 77842, USA

ARTICLE INFO

Article history:
Received 9 December 2015
Received in revised form 26 January 2016
Accepted 27 January 2016
Available online 4 February 2016

Editor: Dr. J. Knight

Keywords:
Phreatic
Karst
Florida
Apalachicola
Underwater cave

ABSTRACT

Detrital sediment in Florida's (USA) submerged cave systems may preserve records of regional climate and hydrologic variability. However, the basic sedimentology, mineralogy, stratigraphic variability, and emplacement history of the successions in Florida's submerged caves remains poorly understood. Here we present stratigraphic, mineralogical, and elemental data on sediment cores from two phreatic cave systems in northwestern Florida (USA), on the Dougherty Karst Plain: Hole in the Wall Cave (HITW) and Twin Cave. Water flowing through these caves is subsurface flow in the Apalachicola River drainage basin, and the caves are located just downstream from Jackson Blue (1st magnitude spring, >2.8 $m^3 s^{-1}$ discharge). Sedimentation in these caves is dominated by three primary sedimentary styles: (i) ferromanganese deposits dominate the basal recovered stratigraphy, which pass upsection into (ii) poorly sorted carbonate sediment, and finally into (iii) fine-grained organic matter (gyttja) deposits. Resolving the emplacement history of the lower stratigraphic units was hampered by a lack of suitable material for radiocarbon dating, but the upper organic-rich deposits have a punctuated depositional history beginning in the earliest Holocene. For example, gyttja primarily accumulated in HITW and Twin Caves from ~5500 to 3500 cal yr. BP, which coincides with regional evidence for water-table rise of the Upper Floridian Aquifer associated with relative sea-level rise in the Gulf of Mexico, and evidence for invigorated drainage through the Apalachicola River drainage basin. Gyttja sediments were also deposited in one of the caves during the Bølling/Allerød climate oscillation. Biologically, these results indicate that some Floridian aquatic cave (stygobitic) ecosystems presently receive minimal organic matter supply in comparison to prehistoric intervals. The pre-Holocene poorly sorted carbonate sediment contains abundant invertebrate fossils, and likely documents a period of enhanced limestone dissolution and cave formation (speleogenesis) during lower paleo water levels. Further work is still required to (a) determine whether precipitation of the ferromanganese deposits is inorganically or biologically mediated, (b) temporally constrain the emplacement history of the primary sedimentary styles, and (c) determine the full geographic extent of these sedimentary signals. However, these preliminary observations suggest that sedimentation in the inland underwater caves of northwestern Florida is related to Quaternary-scale hydrographic variability in the Apalachicola River drainage basin in response to broader ocean and atmospheric forcing.

1. Introduction

Carbonate rocks cover ~12% of the ice-free global surface, and ~25% of the global population is reliant upon freshwater in karst aquifers (Ford and Williams, 1989). However, there remains a poor understanding of how karst aquifers respond to external forcing over millennial timescales, and global freshwater resources are increasingly threatened by climate change and anthropogenic development. Sedimentation in flooded caves may provide a means for assessing the long-term behavior of carbonate aquifers.

In Florida, expansive carbonates were deposited during Oligocene and Eocene sea-level highstands that have since become heavily dissolved into a mature karst landscape with ubiquitous sinkholes, karst windows, and flooded cave systems. Several regional climate records (Watts, 1969; Grimm et al., 1993; Watts and Hansen, 1994; Quillen et al., 2013) and sedimentological studies (Bates et al., 1995; Shinn et al., 1996; Filley et al., 2001; Lane et al., 2011; Brandon et al., 2013) have been focused on Florida's sinkhole sediments, but few studies have examined the sedimentary deposits in Florida's underwater caves and sinkholes to inform regional aquifer development. Alverez Zarikian et al. (2005) used ostracodes preserved in Little Salt Spring to

* Corresponding author at: Department of Marine Sciences, Texas A&M University at Galveston, Galveston, Texas 77554, USA.
E-mail address: vanhenp@tamug.edu (P.J. van Hengstum).

http://dx.doi.org/10.1016/j.sedgeo.2016.01.022
0037-0738/

examine Holocene-scale development of the Upper Floridian Aquifer. Rupert (1991) examined five short push cores collected from the Wakulla Cave System that contained fine-grained carbonate mud and quartz-sand beds (Fig. 1), but resolving their emplacement history was hampered by little chronological control. Martin and Harris (1992) examined the clay mineralogy in three surface sediment samples from Peacock, Telford, and Madison Blue Springs, and Streever (1996) documented organic matter accumulation rates of up to 80 g m^{-2} $yr.^{-1}$ in Sim's Sink Cave. Additional stratigraphic studies are still required to determine the relationship between sediments in Florida's flooded caves and regional ocean and atmospheric forcing.

Here, we present a stratigraphic analysis of two inland phreatic caves on the Dougherty Karst Plain in northwestern Florida (Fig. 1). The objectives of this study were to (i) investigate how sediment mineralogy and texture varies through time, (ii) examine the subsurface stratigraphy and lateral continuity of primary sedimentary units; and (iii) investigate possible temporal relationships between sedimentation, aquifer hydrodynamics, and regional climate change. In short, we recovered ferromanganese deposits from deeper in the stratigraphic record that pass upsection into mixed carbonate sediment and organic matter deposits. Although much remains to be learned, sedimentation in these caves appears linked to water-table rise in the Upper Floridian Aquifer and hydrographic development of the Apalachicola River drainage basin since the last glacial maximum.

1.1. Sedimentation in phreatic caves

Research on underwater cave and sinkhole sediment has significantly expanded in the last several decades from the realization that these deposits can preserve records of paleoceanography (Yamamoto et al., 2010; van Hengstum et al., 2015a), tropical cyclone variability (Lane et al., 2011; Brandon et al., 2013; Denomee et al., 2014; van Hengstum et al., 2014), long-term groundwater conditions and salinity (Teeter and Quick, 1990; Teeter, 1995; Alverez Zarikian et al., 2005; Gabriel, 2009; van Hengstum et al., 2010; Quillen et al., 2013), millennial-scale terrestrial–oceanic climatic connectivity (Grimm et al., 1993), glacial–interglacial climate oscillations (Larsen and Mangerud, 1989), vertical sea level and water level change (van Hengstum et al., 2011; Collins et al., 2015a), and precipitation variability (Wurster et al., 2008; Polk et al., 2013; Onac et al., 2015). However, many questions still surround their millennial-scale sedimentary processes because few flooded caves have received detailed sedimentary reconstructions.

The most significant environmental parameter influencing cave sedimentation is arguably the position (elevation) of the water table with respect to the conduit (in the vadose versus phreatic zone). Inundation by base level due to sea-level rise controls many cave sedimentary processes, and it changes the sedimentary structures that may be generated or preserved in the stratigraphic record. As such, sedimentary deposits and structures (both primary and secondary) can be associated with phreatic versus vadose environmental conditions in the cave (Springer and Kite, 1997; Springer et al., 1997; van Hengstum et al., 2011; Fornós et al., 2014). For example, mud cracks indicate when pre-existing cave sediment has been desiccated under vadose conditions (Fornós et al., 2009; Fornós et al., 2014). Of course, inundation does not necessarily initiate sedimentation in caves, as caves are often dependant upon external sediment supplies (Fornós et al., 2014; van Hengstum et al., 2015b) or conduit geometry (Collins et al., 2015a). For example, a submarine cave at 210 m BSL on

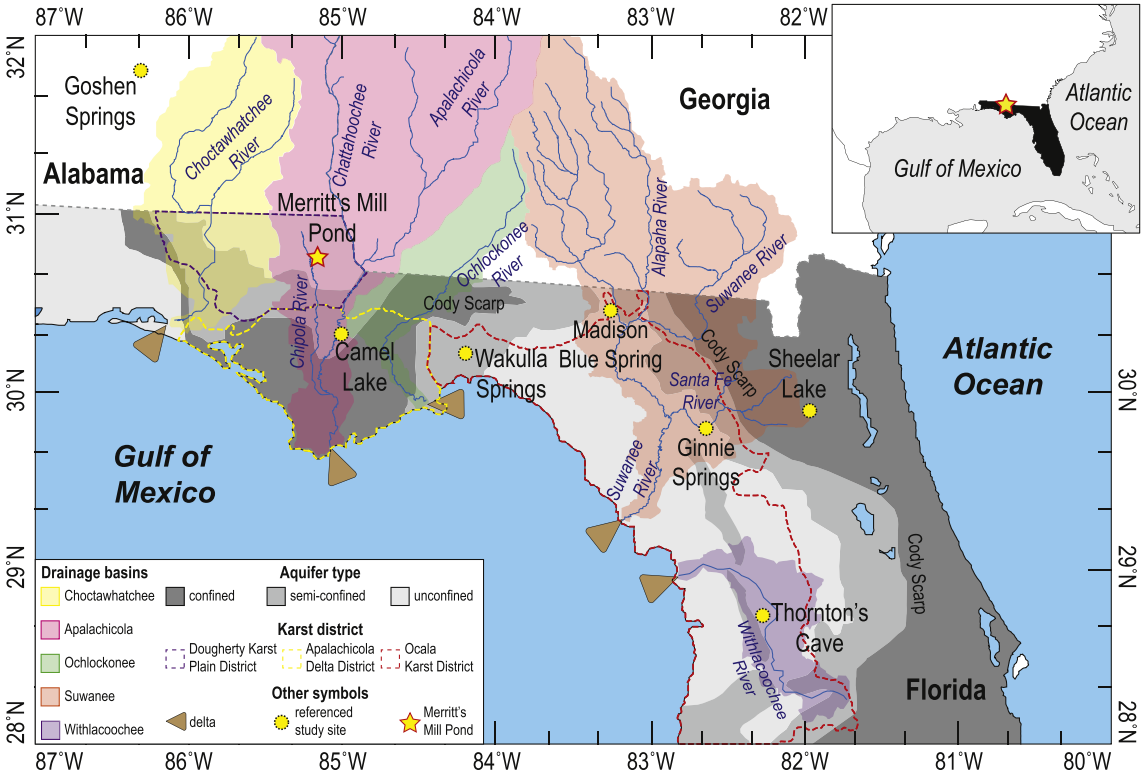

Fig. 1. Map of the major watersheds, streams, deltas, and major geomorphic districts in northern Florida, USA. Hole in the Wall (HITW) Cave and Twin Cave are located along the surficial stream Merrit's Mill Pond (yellow star). Base maps, streams, and the borders of six major drainage basins are modified from multi-resolution topographic (Ryan et al., 2009) and hydrographic databases (Lehner and Grill, 2013), and plotted using GeoMapApp software (http://www.geomapapp.org). Differentiation of confined, semi-confined, and unconfined Floridian aquifers (solid greyscale) is based on a map created by Kurz et al. (2015), as modified from Frydenbourg (2006). The interior border delineating where the upper Florida aquifer is confined (darkest grey) is locally known as the Cody Scarp. Borders of highly karstified geomorphologic districts (constrained by purple, red and yellow dashed lines) are derived from a map by Green et al. (2009). Springs and lakes that have been utilized in paleoclimate, hydrologic, and geologic studies that are referenced herein (yellow circles) include: Goshen Springs (Delcourt, 1980; Grimm et al., 1993), Camel Lake (Watts et al., 1992), Wakulla Springs (Rupert, 1988, 1991), Mud Lake (Watts, 1969), Madison Blue Spring (Brown et al., 2014), Ginnie Springs (Gulley et al., 2013), Sheelar Lake (Watts, 1980), and Thornton's Cave (Florea et al., 2011).

Johnston Island (Central Pacific) contains no sediment (Keating, 1985), and Holocene sedimentation in some Mexican (Yucatan) phreatic caves was initiated by emplacement of mangroves on the epikarst surface (Collins et al., 2015b). The spatial position of the cave system relative to the ocean can further complicate sedimentary interpretations. This is because the position of the water table in the coastal zone is linked to eustatic sea-level change (Gascoyne et al., 1979; Shinn et al., 1996; van Hengstum et al., 2011), whereas the water table is impacted by other variables further inland (e.g., structural geology, lithology, hydrogeologic gradients). Lastly, not all caves will act as sedimentary depocenters throughout time, as conduits can naturally become 'blown-out' and devoid of sedimentation by high rates of water flow.

Most cave sedimentology has been focused on caves located in the modern vadose zone, so cave sediment has been traditionally described and classified as either autochthonous (in situ) or allochthonous (transported). In vadose caves, allochthonous sediments can be delivered through fluvial, aeolian, or biologic vectors (Ford and Williams, 1989; Bosch and White, 2007; White, 2007), whereas weathering products from regional geologic formations, inorganic internal cave geochemical precipitates, or products of biomineralization often provides autochthonous sediment (Onac et al., 1997; Bosch and White, 2007; White, 2007; Fornós et al., 2009; Onac et al., 2014). As research has expanded into phreatic caves, however, it has become apparent that relating sedimentary facies to specific environmental processes is important for accurate paleoenvironmental reconstructions. For example, carbonate mud deposition occurs in coastal submarine caves that are circulated with the ocean (Yamamoto et al., 2010; van Hengstum et al., 2011; van Hengstum et al., 2015a), and calcite rafts precipitate only at modern and paleo water tables (van Hengstum et al., 2011; Collins et al., 2015a).

1.2. Floridian cave systems: lithologic, hydrogeologic, and regional overview

Florida's caves are primarily located within pre-Miocene shallow water carbonates that were primarily deposited in the Eocene (Avon Park Formation and Ocala Limestone) and Oligocene (Suwanee and Marianna Undifferentiated Limestone)(Moore, 1955; Oyen and Protell, 2001). The Avon Park formation is dolomitized peritidal carbonates (Randazzo and Zachos, 1984; Randazzo et al., 1990), the Ocala Limestone is fossiliferous and interbedded with dolostone (Cooke, 1939, 1945; Puri, 1964; Chen, 1965; White, 1970; Schmidt, 1988; Survey et al., 2001), and the Suwanee Limestone is a pale-orange calcarenitic limestone that is also highly fossiliferous (Rupert, 1988). Together, these formations comprise the highly porous and permeable Upper Floridian Aquifer and control regional hydrogeology (Dufresne and Drake, 1999; Martin and Dean, 2001; Jin et al., 2014). Depending on regional thickness of the post-Miocene siliciclastics, especially the Hawthorne Group, the Upper Floridian Aquifer can be confined, semi-confined or unconfined (Fig. 1).

Florida has three primary karst areas: the Ocala Karst District near the Suwanee River drainage basin (Ocala limestone), the Apalachicola Delta District (Suwanee Limestone) (Rupert, 1988; Schmidt, 1988), and the Dougherty Karst Plain District in the Apalachicola River drainage basin (combination of Ocala and Suwanee Limestone) (Spencer and Lloyd, 1999; Green et al., 2009) (Fig. 1). In the Suwanee River drainage basin (25,800 km^2), the Upper Floridian Aquifer is confined in the north and east by the siliciclastic Hawthorn Group until its erosional edge at the Cody Scarp when the aquifer becomes unconfined (Fig. 1). This regional geologic variability provides an excellent natural laboratory to study the relationships between hydrogeologic variability of the Upper Floridian Aquifer, regional karstification, and subsurface mineralization (Florea et al., 2011; Gulley et al., 2013; Brown et al., 2014). The Suwannee River has eroded an incised channel to a maximum depth of only 9 m below modern sea level that extends 15 km out from the shoreline into the Gulf of Mexico, and it has only produced a modest Holocene delta (<20 km^2) (Wright et al., 2005). This starkly contrasts with the deep incised valley systems and deltas produced by rivers on the siliciclastic coastlines in the northwestern Gulf of Mexico (e.g., Brazos and Trinity Rivers) during the Last Glacial Maximum (Anderson et al., 2008). Gulley et al. (2013) describes how the modern surficial drainage through the lower Suwanee River drainage basin was only activated after Holocene sea-level rise forced vertical migration of the Upper Floridian Aquifer into channel systems in the unconfined carbonates. The Upper Floridian Aquifer is also unconfined in the Marianna Lowlands (Cooke, 1945), or Dougherty Karst Plain (Spencer and Lloyd, 1999), and this region is connected into the Apalachicola River drainage basin. The Apalachicola River has produced a modern bayhead delta in Apalachicola Bay that formed ~8000 years ago (Osterman et al., 2009; Twichell et al., 2010).

Two primary groups of hypotheses are generally used to describe the formation of Florida's submerged caves (Gulley et al., 2013). First, one group of hypotheses suggest that Floridian caves formed from groundwater conditions analogous to other global localities where caves are currently being formed, such as dissolution from either sinking streams (Palmer, 2007), or mixing of different water masses that allowed the mixed water to become undersaturated with respect to calcite and dissolve limestone (Rhoades and Sinacori, 1941; Brinkmann and Reeder, 1994). In contrast, the second group of ideas suggest that Floridian phreatic caves formed under hydrogeologic conditions not analogous to the present when water tables were lower during glacioeustatic regressions (Florea et al., 2007; Gulley et al., 2011; Gulley et al., 2013). As discussed by Gulley et al. (2013), Holocene sea-level rise, shoreline migration in the Gulf of Mexico, and concomitant base-level rise of the Upper Floridian Aquifer would have eventually (i) submerged Florida's cave systems, (ii) activated the present highstand hydrography of the Suwanee River System, and (iii) initiated delta formation in the Gulf of Mexico. Perhaps these previously addressed linkages between oceanography, geomorphology, and hydrogeology in the Suwanee River drainage basin are also important in the northwestern region of Florida.

2. Study site

Hole in the Wall Cave (HITW; N 30.78327°, W 085.15618° ± 3 m) and Twin Cave (N 30.78691°, W 085.14494° ± 3 m) are located ~300 m apart in Merritt's Mill Pond on the Dougherty Karst Plain, Florida (Figs. 1, 2). Merritt's Mill Pond is a surface stream feature (1.1 km^2) that is fed at its northeastern end by the discharge of Jackson Blue, a magnitude 1 spring with a discharge of >2.8 $m^3\ s^{-1}$ (Fig. 2). Merritt's Mill Pond has been dammed several times since the 1880s to accommodate local agricultural activities (Dodson, 2013), but it hydrographically contributes to the Apalachicola River drainage basin through smaller tributaries (e.g., Spring Creek, Chipola River). Groundwater flooding HITW Cave and Twin Cave is currently homogenized freshwater that is pH neutral and well oxidized. HITW Cave has a mean temperature of 20.4 ± 0.1 °C, a mean salinity of 0.15 ± 0.01 psu, a mean pH of 7.2 ± 0.1, and a mean dissolved oxygen concentration of 5.7 mg/L ± 0.2. Similarly, Twin Cave has a mean temperature of 20.3 ± 0.2 °C, a mean salinity of 0.2 ± 0.1 psu, a mean pH of 7.2 ± 0.3, and a mean dissolved oxygen concentration of 5.9 ± 0.6 mg/L. The light-limited cavern area in both caves has variable and discontinuous sediment (quartz sand, coarse organic matter, freshwater mollusk shells), but this often transitions to fine-grained organic matter (gyttja) with increasing penetration into the caves.

The conduit geometry and geographic position on the stream channel differ for each cave. Twin Cave occurs in the center of Merritt's Mill Pond, and is more proximal to Jackson Blue Spring (1st magnitude spring) than HITW Cave (Fig. 2). Twin Cave has a larger entrance and the conduits have a clear two-story pattern: horizontally extensive conduits occur primarily at ~16 m and ~28 m below the modern water table that are connected by vertical conduits or 'chimneys' (Fig. 3). In contrast, HITW Cave is located further downstream from Twin

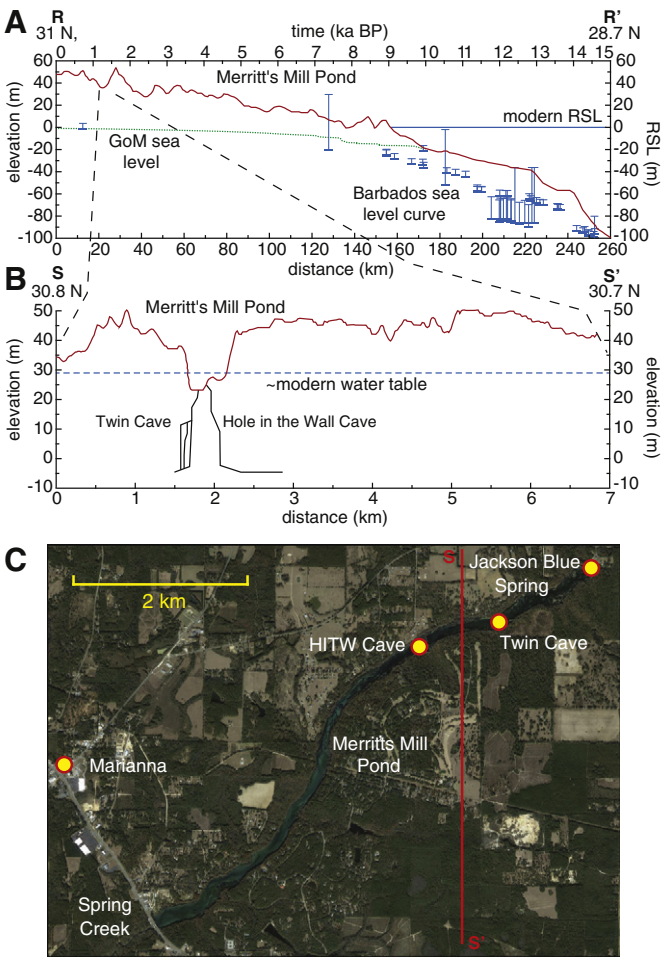

Fig. 2. (A) Topographic profile from the Gulf of Mexico to the study site (red line). A framework for deglacial sea-level rise is provided by relative sea-level change in the gulf of Mexico in green (Milliken et al., 2008), and blue data points are far-field coral-based sea-level index points (Peltier and Fairbanks, 2006). (B) Detailed cross-section through the Meritts Mill Pond stream channel (red line). (C) Landsat image of the study site, with the magnitude 1 spring (Jackson Blue) in the top right. Both topographic profiles were generated using multi-resolution topographic data in (Ryan et al., 2009) GeoMapApp software.

Cave (Fig. 2), it is located on the stream channel margin, and it is accessed by a narrow karst window. The conduits in HITW Cave that are proximal to the karst window have a roughly linear geometry and trend towards the northeast. The typical depth to the sediment–water interface in HITW Cave is 26 to 30 m below the modern water level.

3. Methods

Sediment push cores were collected using advanced technical cave diving procedures on May 2011 and July 2014: five cores from HITW Cave and six from Twin Cave (Figs. 3, 4). Core depths were measured with respect to modern water table elevation (±0.3 m), and no attempt was made to reference the current inland water table elevation to present sea level in the Gulf of Mexico. Sediment cores were collected using 5 or 8 cm diameter and 2.4 m length clear polycarbonate pipes, while following safety protocols exceeding those outlined by the American Academy of Underwater Sciences (AAUS). Coring sites were separated by approximately 60 m of horizontal cave passage at water depths ranging from 15 to 30 m below the modern water table. Thick sediment (>2.4 m) has accumulated in the surveyed areas of HITW Cave, but sediment accumulation was more limited in Twin Cave as bedrock was reached on all coring drives except TWIN-C1 (Table 1, Fig. 3). After extraction, cores were transported back to the laboratory where they were split lengthwise, photographed, stratigraphically described according to texture and the 2009 Year (revised 2012) *Munsell Soil Color Book*, and continuously stored at 4 °C until further analysis.

Textural variability was analyzed in all cores using a modified loss on ignition procedure (Sieve-First LOI, van Hengstum et al., 2016) and laser particle size determination. For Sieve-First LOI, contiguous sediment subsamples (2.5 cm^3) were wet-sieved over a 63-μm mesh, emptied into pre-weighed ceramic crucibles, and dried in an oven 80 °C for 12 h or until dry. After samples were dried and re-weighed, the remaining organic matter in the samples was ignited in a muffle furnace at 550 °C for 4.5 h. Each crucible and remaining sediment residue was then re-weighed to determine a final mass in milligrams of coarse sedimentary particles exceeding 63 μm in diameter per unit cm^3 (note: expressed throughout as $D_{>63\ um}$ mg cm^{-3}, which is not density). To determine bulk organic matter, a separate set of sediment samples were exposed to a classic loss on ignition procedure, following standard methods (Dean, 1974; Heiri et al., 2001). However, it is likely that organic matter is overestimated in sedimentary units rich in oxide and hydroxide minerals (Boyle, 2004). Textural variability was further quantified in HITW-C1 with a Malvern Mastersizer 2000 laser diffraction particle size analyzer to measure standard particle size statistics (volumetric mean, standard deviation, mode). The resultant particle size distributions were interpolated and displayed using a color surface plot (Fig. 5).

The mineralogy and trace element variability was examined with XRF core scanning and X-ray diffraction (XRD). All recovered sedimentary units are represented in HITW-C1, so this core was scanned on a non-destructive Itrax core scanner every 250 μm to obtain relative X-ray fluorescence measurements of the sediment's elemental composition. A further 19 sediment subsamples from specific sedimentary units were selected for XRD analysis (HITW-C1, C2; TWIN-C1, C4, C5, C6). XRD data was measured on a Bruker-AXS D8 Advanced Bragg–Brentano X-ray powder diffractometer employing standard XRD laboratory protocols. The minerals in each sample were determined by comparing resultant diffractograms with the 2005 International Center for Diffraction Data (ICDD) material identification database (Fawcett et al., 2005).

Age control was established by radiocarbon dating organic matter remains with accelerator mass spectrometry. Samples of bulk organic matter were submitted for radiocarbon dating because discernable plant macrofossils (e.g., twigs, leaves) were only present in the cores directly adjacent to the subaerial cave opening (karst windows). We assume the primary source of allochthonous organic matter in the cave is the adjacent terrestrial surface. Nine bulk organic matter samples from TWIN-C1, TWIN-C4, HITW-C1, and HITW-C2 and a twig from TWIN-C3 were submitted to National Ocean Sciences Accelerator Mass Spectrometry. Final conventional radiocarbon dates were calibrated to calendar years before present (cal yr. BP) with IntCal13 (Reimer et al., 2013) using the freeware program CALIB 7.1 to account for secular changes in atmospheric radiocarbon concentrations (Table 3).

4. Sedimentary units

4.1. Organic matter deposits (Unit 1)

Unit 1 in both caves is dominated by bulk organic matter (30 ± 11%, $n = 424$) that is 'black' (10YR 2/1) with occasional 'brownish yellow' (10YR 6/8) laminations. This facies in HITW-C1 (0–37 cm) is dominated by coarse to medium silt with a mean particle size of 55 ± 14 μm (4–5 ϕ) (Table 2; Fig. 5), and the average coarse particle content for the facies ($D_{<63\ um}$) was 8 ± 9 mg cm^{-3} ($n = 340$). Coarser-grained horizons are occasionally present (e.g., 35 to 36 cm in HITW-C2) that contain marine invertebrate fossils (e.g., echinoid spines, marine foraminifera) that eroded out from the host limestone bedrock. The unit

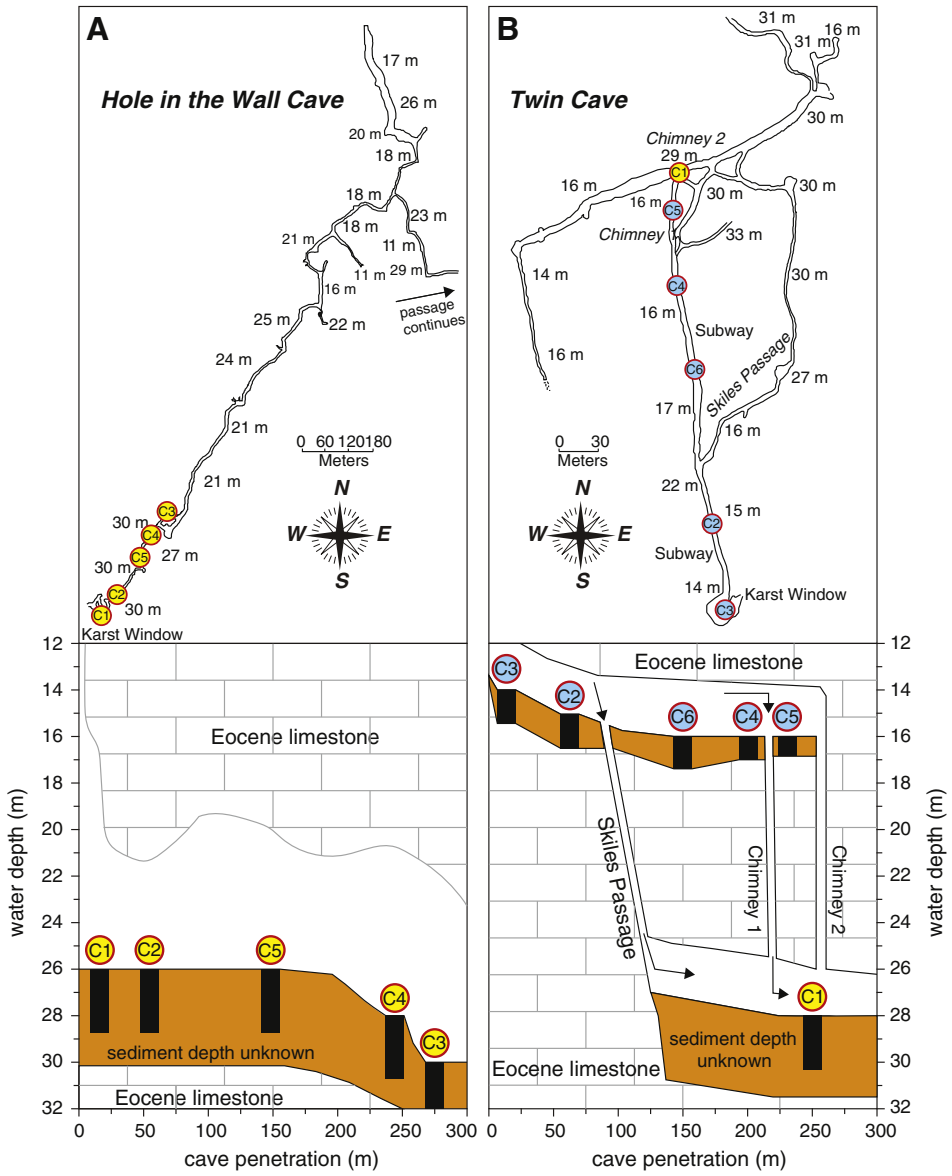

Fig. 3. Original cave surveys (top panel, after original by Sheck Exley) denoting core locations, along with idealized cave cross section with core depths (lower panel) from HITW Cave (A) and Twin Cave (B). Black bars denote original sediment column before compression occurred during coring (not recovered length, Table 1). Blue (yellow) circles denote cores that reached (did not reach) bedrock. Note: 'Sediment bypass' down Chimney 1 and/or the Skiles Passage likely precluded deposition of organic matter pulses (OMP-1, OMP-2) in TWIN-C5 (see Fig. 4).

generally contains a low abundance of Fe and Mn (Fig. 5), but narrow increases in Mn correlate to narrow 'brownish yellow' (10YR 6/8) laminations (e.g., 26 to 37 cm, HITW-C1). A 'yellowish red' (5YR 4/6) horizon (<3 cm) occurred near the sediment–water interface in all HITW Cave cores (Fig. 6A), which the XRD results from HITW-C4 (3–4 cm) indicate that this is from the presence of goethite ($Fe_3(O)OH$) and birnessite ($(Na_{0.3}Ca_{0.1}K_{0.1})(Mn)_2O_4$) (Fig. 7).

The lateral continuity and net accumulation of Unit 1 differs between each cave. The uppermost 35–75 cm of sediment in all cores from HITW Cave contains a texturally similar unit 1. In contrast, Unit 1 in Twin Cave was primarily fine-grained (gyttja), except near the karst window (TWIN-C3) where coarse-grained organic fragments and freshwater gastropod shells were abundant (Figs. 4, 5). More distally into Twin Cave, Unit 1 attenuates into a thin layer (<5 cm) that is texturally similar to HITW Cave. Lastly, TWIN-C1 was obtained from the base of the vertical shaft connecting the upper and lower horizontal conduit levels. Unit 1 occurred as a thin deposit at top of TWIN-C1 (<5 cm), but also as a thick sequence from 22 to 65 cm depth (Fig. 4). This lower deposit contains more intact and leafy organic matter particles in an overall fine-grained organic matter matrix.

4.2. Carbonate sediment (Unit 2)

This facies is present in both HITW Cave and Twin Cave, and is dominated by poorly sorted carbonate particles with low bulk organic matter content (4 ± 3% bulk organic matter, $n = 442$). The facies was subdivided because of its heterogeneous texture (Units 2A and 2B, Figs. 4-6). Unit 2A can range from 'yellow' (10YR 8/6) to 'strong brown' (7.5YR 4/6), and Unit 2B is 'very pale brown' (10YR 8/3) to 'brownish yellow' (10YR 6/8). Based on particle size analysis of HITW-C1, Unit 2A contains intervals of fine-grained sandy-silt (4 to 8 ϕ) with a mean particle size of 53 ± 19 μm ($n = 11$, 38 to 49 cm:) whereas Unit 2B is fine to medium sand (0 to 3 ϕ) with a mean particle size of 292 ± 111 μm ($n = 12$, 49 to 60 cm). The coarser sediment particles in Unit 2B are typically lithified marine fossils (e.g., echinoid spines, ichthyoid tooth) and carbonate rock particles. The sieve-first LOI

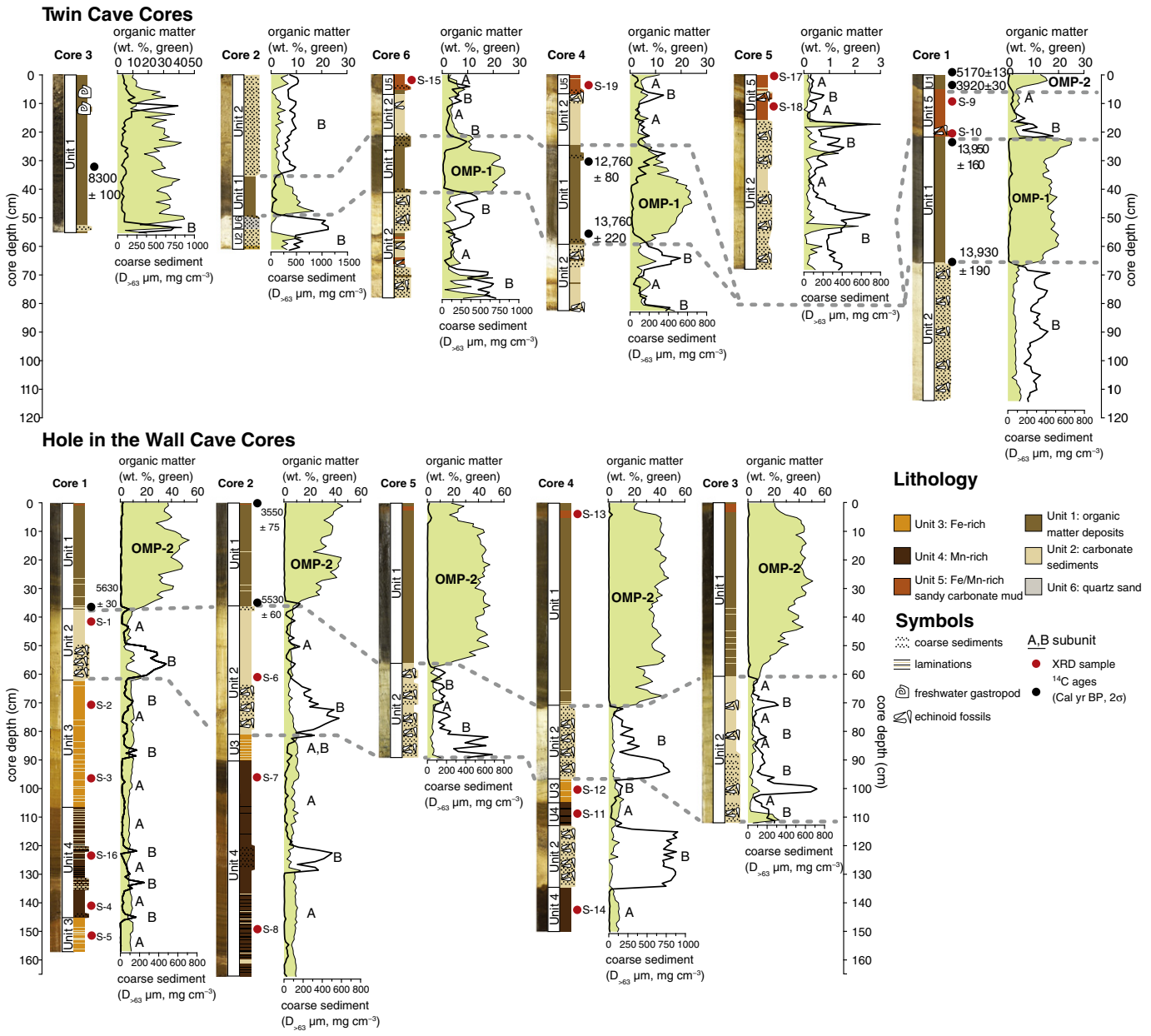

Fig. 4. Lithologic variability (core logs and photographs), bulk organic matter (wt. %), coarse sediment fraction ($D_{>63\ \mu m}$), location of XRD and ^{14}C samples in all of the recovered cores.

Table 1
Summary of coring locations and sediment recovery from Hole in the Wall Cave and Twin Cave (N/R = not recorded).

Core	Horizontal cave penetration (m)	Water depth (m)	Stratigraphic column sampled (cm)	Compressed sediment recovery (cm)	Basement reached (Y/N)
HITW-C1	15	26	240	157	N
HITW-C2	50	26	240	166	N
HITW-C3	274	30	150	111.5	N
HITW-C4	244	28	235	150.5	N
HITW-C5	137	26	240	88	N
TWIN-C1	250	28	220	113	N
TWIN-C2	60	15	*N/R	60	Y
TWIN-C3	10	14	150	56.5	Y
TWIN-C4	200	16	102	82	Y
TWIN-C5	230	16	77	68	Y
TWIN-C6	150	16	131	78	Y

technique that examined the coarse fraction also indicates the textural heterogeneity of Unit 2, as the coarse sediment fraction ($D_{>63\ \mu m}$) varies between 16 and 118 mg cm^{-3} (mean: 73 ± 28 mg cm^{-3}, $n = 116$) in Unit 2A and from 120 to 993 mg cm^{-3} (mean: 350 ± 191 mg cm^{-3}, $n = 326$) in Unit 2B.

XRF elemental analysis indicates a high abundance of Ca and Sr in Unit 2, with a low abundance of Fe and Mn (Fig. 5). XRD analysis of samples from Unit 2 indicate that calcite ($CaCO_3$) and quartz (SiO_2) were the most dominant minerals, which supports the XRF results (Table 2; Figs. 5, 7). However, goethite ($Fe_3(O)OH$), magnetite (Fe_3O_4), and trace amounts of kaolinite ($Al_2Si_2O_5(OH)_4$) were also detected (Table 2; Fig. 7). No evidence of desiccation was observed (e.g., mudcracks).

4.3. Fine-grained iron-rich facies (Unit 3)

Unit 3 is a laminated and Fe-rich (Fig. 5) unit that contains an average of ~9 ± 2% bulk organic matter, but this is likely an overestimate

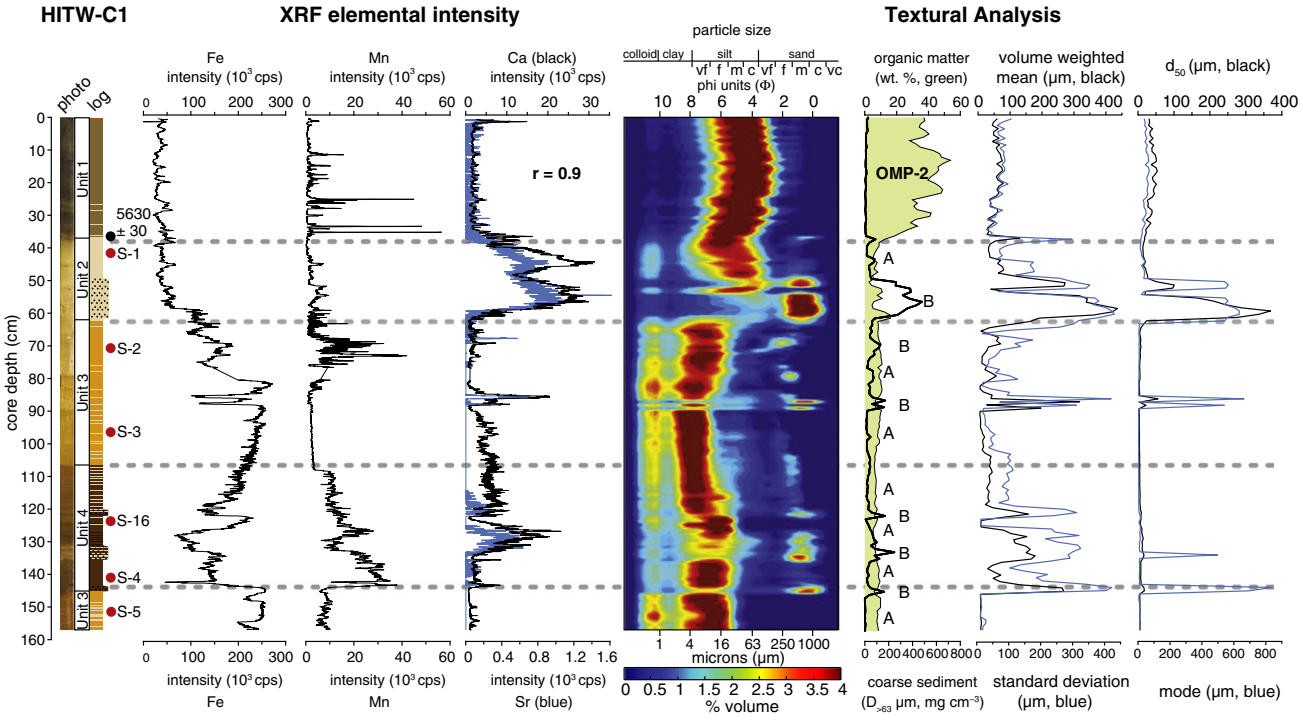

Fig. 5. Detailed elemental (Fe, Mn, Ca, and Sr) and textural variability in HITW-C1. Intervals with increased coarse-grained particles in Units 3 and 4 (prominent features in the interpolated particle size distribution) are from increased concentration of fossil invertebrates that have eroded out of the host carbonate. See Fig. 4 for symbols.

given the high content of oxide minerals (Boyle, 2004). The negligible lower amount of Mn in Unit 3 differentiates it from Unit 4. In general, Unit 3 is dominated by silt and clay particles (mean particle size: 9 ± 3 μm, 6 to 10 ϕ, $n = 28$) with coarser-grained sand horizons. So, we further subdivided Unit 3 into subunits based on the content of coarse particles (Figs. 4-6). Subunit 3A contains a mean coarse sediment fraction ($D_{>63\ \mu m}$) of ~23 ± 16 mg cm^{-3} ($n = 46$), but Unit 3B has a mean coarse sediment fraction of ~101 ± 41 mg cm^{-3} ($n = 29$) (Figs. 4-6). No evidence of desiccation was observed in this unit (e.g., induration crusts, mudcracks). Based on XRD analyses on a sample of Unit 3 from HITW-C1, the minerals goethite ($Fe_3(O)OH$), magnetite (Fe_3O_4), calcite ($CaCO_3$), and quartz (SiO_2) are present (Fig. 7). It is noteworthy that 'yellow' (10YR 7/8) laminations in the sediment appear to correlate with increased abundance of Ca in HITW-C1, and 'dark brown' (7.5YR 2.5/3) laminations appear to correlate with increased Mn abundance (Fig. 5).

4.4. Intercalated Mn- and Fe-oxides (Unit 4)

Only HITW Cave cores contain Unit 4, which has higher Mn content than the other units (Fig. 5) and is laminated (Figs. 4,6A). Bulk organic matter content is estimated at 8 ± 2% ($n = 135$), but this is likely an overestimate based on the high content of ferromanganese minerals. One layer dominated by Mn in Unit 4 was exceptionally dark in color ('dark brown', 7.5YR 2.5/2), which could be correlated between several cores in HITW Cave (e.g., HITW-C1: 132–142 cm, HITW-C2: 90–101 cm, HITW-C4: 134–150 cm). Large accumulations of Mn-dominated cave sediments have been previously documented, such as the 3 m successions of manganese oxide sediments in the lowest conduit levels in Jewel Cave, South Dakota (Hill, 1982; Peck, 1986). Unit 4 is also divided into subunits based on the textural variability. Unit 4A contains well-sorted fine to coarse silt (8 to 4 ϕ, Unit 4 A), but Unit 4B contains medium to coarse sand layers (2 to 0 ϕ) with invertebrate fossil grains and carbonate sand particles (Figs. 4-6).

Though the precise mineralogical structure of naturally precipitated Mn oxides and oxyhydroxides can be difficult to determine due to their extreme microcrystallinity (Lind et al., 1987; Davison, 1993), the intensity of the correlated peaks in the XRD diffractograms would suggest that birnessite ($(Na_{0.3}Ca_{0.1}K_{0.1})(Mn)_2O_4$), jacobsite ($MnFe_2O_4$), and ramsdellite ($MnO_2$) dominate Unit 4 (Table 1, Figs. 6, 7). XRD results indicate that goethite ($Fe_3(O)OH$), calcite ($CaCO_3$), and quartz (SiO_2) (Table 2; Fig. 7) are also present. Similar to Unit 3, XRF scans of HITW-C1 reveal alternating 'yellow' (10YR 7/8) and 'black' (10YR 2/1) fine-grained laminations throughout most of Unit 4 sediments that correlate to increased levels of Ca in the sediment (Fig. 5).

4.5. Ferromanganese-rich sandy carbonate mud (Unit 5)

Unit 5 only occurs in Twin Cave (TWIN-C1, C4, C5, and C6) and it is highly heterogeneous in terms of coarse sediment (>63 μm) and mineralogy. It would visually appear to be a variant of Unit 2 (carbonate sediment), but it contains additional layers that are rich in ferromagnesian minerals. This is evidenced by the sediment color, which was 'dark reddish brown' (5YR 3/4) with occasional 'dark brown' (7.5YR 2.5/2) laminations, or vice versa. The particle size in Unit 5 varies from clay to coarse sand (10 to 0 ϕ), so the unit was further divided into subunits (Units 5A and 5B) based on bimodal distribution of coarse sediment fraction ($D_{>63\ \mu m}$) data. Unit 5A is dominated by silt and clay with a mean coarse sediment fraction of 64 ± 21 mg cm^{-3} ($n = 30$), whereas Unit 5B is comprised of fine to medium sand with a mean coarse sediment fraction of 214 ± 101 mg cm^{-3} ($n = 17$). Organic matter content in both subunits was generally very low with a mean composition of 3 ± 2% ($n = 46$) (Table 2; Fig. 5).

The results of the XRD analysis indicate inconsistent trace metal and mineralogical characteristics for this unit. Overall, crystalline minerals such as calcite ($CaCO_3$) and quartz (SiO_2) appear to be the most dominant; however, there is also a very strong presence of Fe and Mn oxides and oxyhydroxide minerals including goethite ($Fe_3(O)OH$), magnetite (Fe_3O_4), birnessite ($(Na_{0.3}Ca_{0.1}K_{0.1})(Mn)_2O_4$), jacobsite ($MnFe_2O_4$), and ramsdellite ($MnO_2$) as well as trace amounts of kaolinite ($Al_2Si_2O_5(OH)_4$) (Fig. 7). In fact, this facies contains

Table 2
Primary textural and mineralogical characteristics of recovered sedimentary units.

Unit	Sedimentary description	Grain size (HITW-C1)	Coarse sediment fraction ($D_{>63\ \mu m}$)	Organic matter (% weight)	Fossils	Munsell color	Mineralogy
1	*Organic matter deposits* -OMP-2: medium silts -OMP-1: fibrous OM in a silt matrix Occasional coarse horizons and a <5 cm redox boundary at sediment–water interface	Unit 1: *Mean*: 55 ± 14 μm, 4–5 ϕ *Sample STDEV*: 65 μm $n = 37$	5 ± 33 mg cm^{-3} in 80% of samples $n = 340$	30 ± 11% $n = 424$	Rare freshwater gastropod shells Rare Eocene echinoid spines and marine foraminifera in coarse horizons	*General*: 'Black' (10YR 2/1) *Laminations*: 'Brownish yellow' (10YR 6/8) *Redox*: 'Yellowish red' (5YR 4/6)	Bulk organic matter *Redox*: Goethite (Fe(O)OH) Birnessite ($(Na_{0.3}Ca_{0.1}K_{0.1})(Mn)_2O_4$) Calcite ($CaCO_3$) Quartz ($SiO_2$)
2	*Carbonate sediments* Poorly sorted Unit 2A: fine sandy silts Unit 2B: predominantly coarse fossiliferous sand in a silt matrix	Unit 2A: *Mean*: 53 ± 19 μm, 4–8 ϕ *Sample STDEV*: 65 μm $n = 11$ Unit 2B: Mean: 292 ± 111 μm, 0–3 ϕ *Sample STDEV*: 348 μm $n = 12$	Unit 2A: <120 mg cm^{-3} 73 ± 28 mg cm^{-3} $n = 120$ Unit 2B: >120 mg cm^{-3} 350 ± 191 mg cm^{-3} $n = 332$	4 ± 3% $n = 450$	Abundant Eocene marine fossils: -echinoid spines and fragments -foraminifera	Unit 2A *General*: 'Yellow' (10YR 8/6) to 'Strong brown' (7.5YR 4/6) Unit 2B *General*: 'Brownish yellow' (10YR 6/8)	Calcite ($CaCO_3$) Quartz (SiO_2) Goethite (Fe(O)OH) Magnetite (Fe_3O_4) Kaolinite ($Al_2Si_2O_5(OH)_4$)
3	*Fine-grained iron-rich facies* Unit 3 A: fine silt and clay matrix-highly laminated Unit 3B: medium sand in a silty-clay matrix	Unit 3 A: *Mean*: 9 ± 3 μm, 6–10 ϕ *Sample STDEV*: 19 μm $n = 28$ Unit 3B: *Mean*: 131 ± 109 μm, 0–3 ϕ *Sample STDEV*: 215 μm $n = 13$	Unit 3 A: <50 mg cm^{-3} 23 ± 16 mg cm^{-3} $n = 46$ Unit 3B: >50 mg cm^{-3} 101 ± 41 mg cm^{-3} $n = 29$	9 ± 2% $n = 74$	Rare Eocene marine fossils: -echinoid spines and fragments -foraminifera	*General*: 'Strong brown' (7.5YR 4/6) *Laminations*: 'Yellow' (10YR 7/8)	Goethite (Fe(O)OH) Magnetite (Fe_3O_4) Calcite ($CaCO_3$) Quartz (SiO_2)
4	*Intercalated Mn- and Fe-oxides* Unit 4 A: silt and clay matrix-highly laminated Unit 4B: medium sand in a silty-clay matrix	Unit 4 A: *Mean*: 33 ± 12 μm, 4–8 ϕ *Sample STDEV*: 89 μm $n = 21$ Unit 4B: *Mean*: 136 ± 61 μm, 0–3 ϕ *Sample STDEV*: 280 μm $n = 19$	Unit 4 A: <50 mg cm^{-3} 23 ± 16 mg cm^{-3} $n = 109$ Unit 4B: >50 mg cm^{-3} *Peak 1*: 95 ± 41 mg cm^{-3} $n = 20$ *Peak 2*: 372 ± 81 mg cm^{-3} $n = 8$	8 ± 2% $n = 135$	Rare Eocene marine fossils: -echinoid spines and fragments -foraminifera	*General*: 'Very dark brown' (7.5YR 2.5/2) *Laminations*: 'Yellow' (10YR 7/8) 'Black' (10YR 2/1)	Birnessite ($(Na_{0.3}Ca_{0.1}K_{0.1})(Mn)_2O_4$) Jacobsite ($MnFe_2O_4$) Goethite (Fe(O)OH) Calcite ($CaCO_3$) Quartz (SiO_2)
5	*Ferromanganese-rich sandy carbonate mud* Unit 5 A: fine carbonate sand in an Fe/Mn rich silt matrix Unit 5B: coarse sand in an Fe/Mn rich silt matrix	Not sampled	Unit 5 A: <120 mg cm^{-3} 64 ± 21 mg cm^{-3} $n = 30$ Unit 5B: >120 mg cm^{-3} 214 ± 101 mg cm^{-3} $n = 17$	3 ± 2% $n = 47$	Some Eocene marine fossils: -echinoid spines and fragments -foraminifera	*General*: 'Dark reddish brown' (5YR 3/4) *Laminations*: 'Dark brown' (7.5YR 2.5/3) 'Brownish yellow' (10YR 6/8)	Goethite (Fe(O)OH) Calcite ($CaCO_3$) Quartz (SiO_2) Birnessite ($(Na_{0.3}Ca_{0.1}K_{0.1})(Mn)_2O_4$) Jacobsite ($MnFe_2O_4$)
6	Coarse quartz sand Very well sorted	Not sampled	1074 ± 59 mg cm^{-3} $n = 5$	<1 ± 1% $n = 5$	No apparent fossils	*General*: 'White' (10YR 8/1)	Silica sand: Quartz (SiO_2)

discernable levels of every mineral identified in each of the other facies identified in Units 2–4.

4.6. Quartz sand (Unit 6)

Unit 6 is well-sorted, 'white' quartz sand (10YR 8/1). This facies is only present in TWIN-C2 at 49 to 54 cm, just before deposition of Unit 1. Sediment from this unit was too coarse to be analyzed by XRD; however, exposure of the sand-sized particles to 10% HCl produced no effervescence. This suggests the sand is most likely quartz (SiO_2). This unit also contained little organic matter (>1 ± 1%), and has the highest mean coarse sediment (>63 μm) fraction of all of the observed facies (1074 ± 59 mg cm^{-3}) (Table 2; Fig. 4). No fossil material was observed.

5. Chronology and correlation

Based on the textural and mineralogical characteristics, the facies can be grouped into three broad sedimentary styles, in stratigraphic order from bottom to top: *ferromanganese deposits* (Units 3, 4), *carbonate sediment* (Unit 2), and *organic matter deposits* (Unit 1). Aside from the bulk organic matter deposit (Unit 1), there was no substantial organic material in Units 2–6 for radiocarbon dating (i.e., terrestrial plant macrofossils, reliable bulk organic matter), which hampered a direct interpretation for the timing of their emplacement. However, they must have been emplaced during the late Pleistocene given the oldest radiocarbon dates obtained from TWIN-C1 (Table 3).

Based on the longer cores from HITW Cave, the basal and presumably oldest facies are the ferromanganese deposits. The recovered stratigraphy from Twin Cave is missing the thick ferromanganese deposits that are present in HITW Cave, but this may be an artifact of the research design since there are many conduits in Twin Cave that were not sampled. The ferromanganese deposits can be correlated between the cores collected from HITW cave, and are likely derived from a similar environmental emplacement mechanism given their similar character. Indeed, dating the transition between the ferromanganese deposits and carbonate sediment is critical to resolving uncertainty regarding its emplacement history, but nevertheless, this salient sedimentary contact warrants correlation in the subsurface.

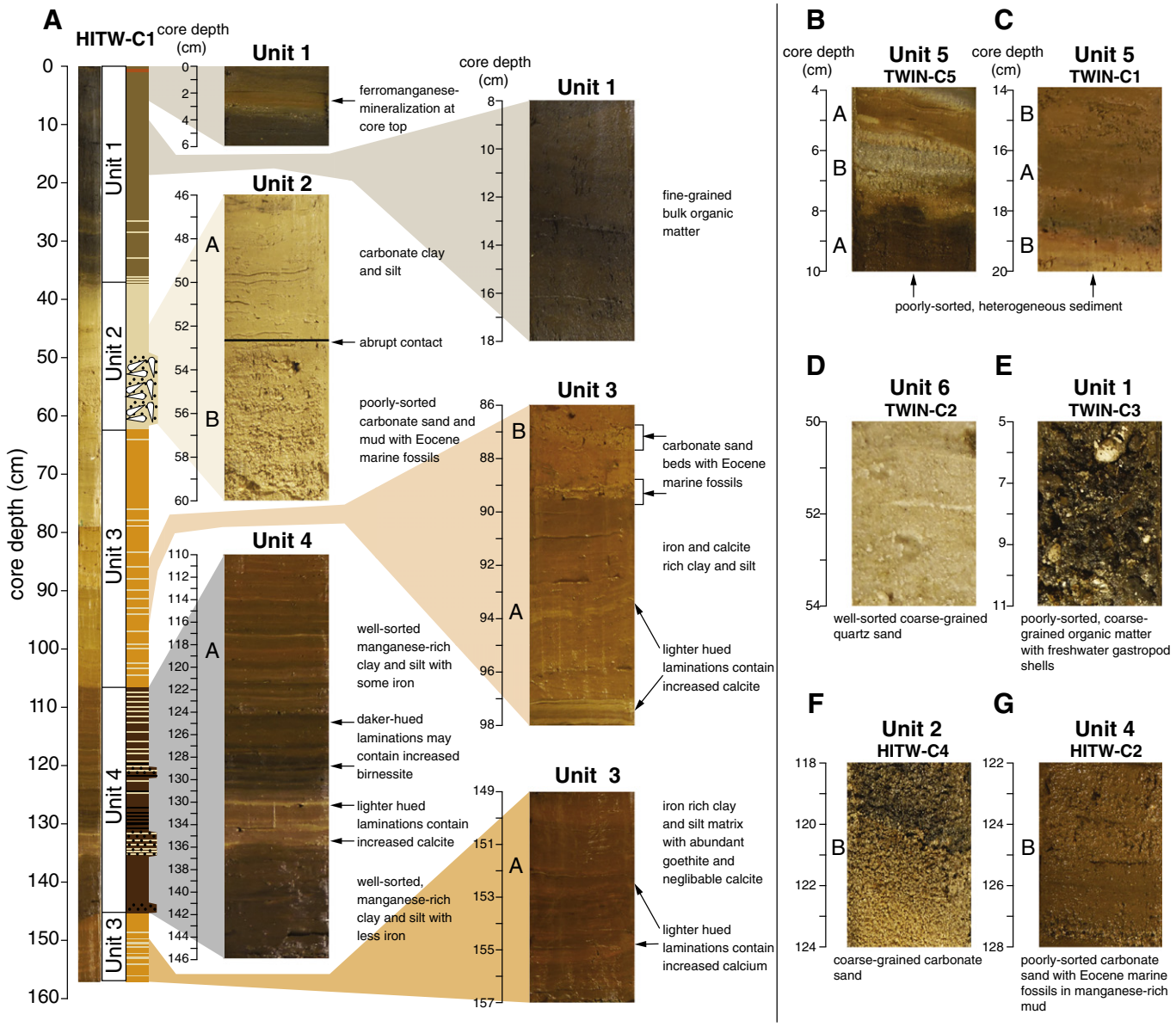

Fig. 6. (A) Photographs from HITW-C1 depicting sediment typical of Units 1–6. (B, C) Photographs from TWIN-C5 and TWIN-C1 (respectively) that depict the heterogeneity of Unit 5 sediment. (D) Well-sorted, coarse quartz sand from Unit 6 in TWIN-C2. (E) Poorly sorted, coarse-grained Unit 1 from TWIN-C3. (F) Unit-2B coarse-grained carbonate sand from HITW-C4 that is well-sorted unlike most Unit 2B sediment. (G) Poorly sorted carbonate sand in manganese-rich mud from HITW-C2 that is typical of Unit 4B.

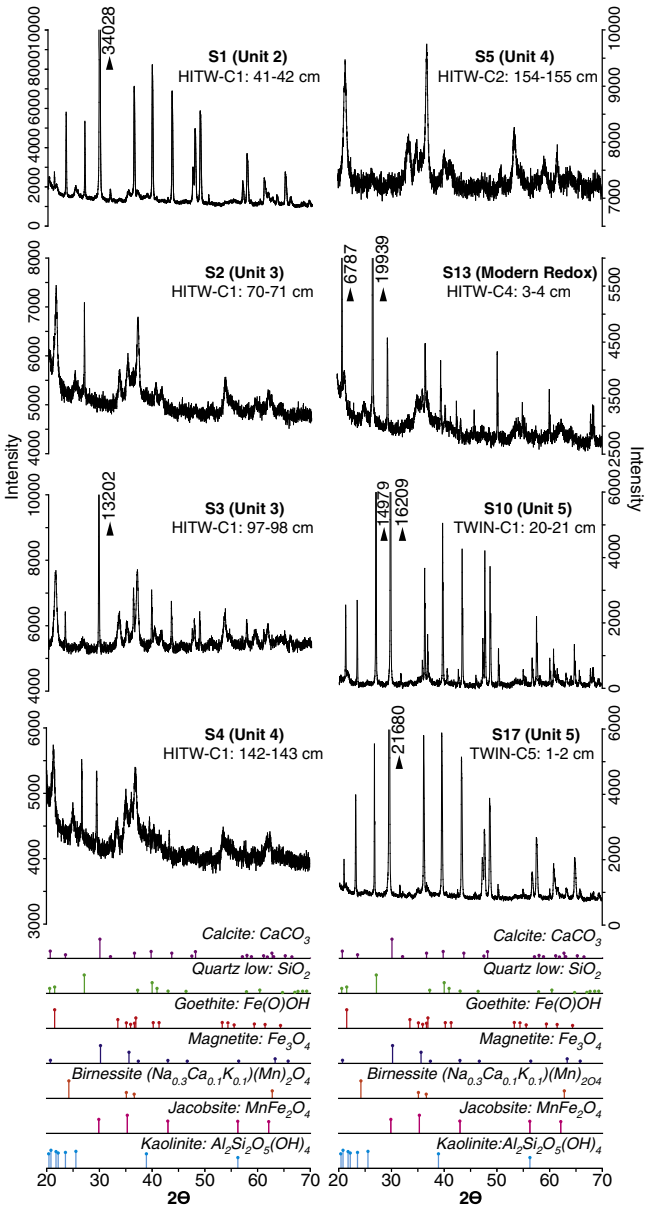

Fig. 7. XRD results from representative sedimentary units 1–5 (Figs. 3, 4) in HITW Cave and Twin Cave. Reference peaks for minerals are identified below (stick graphs after Fawcett et al., 2005).

In HITW Cave, the ferromanganese deposits pass upwards into carbonate sediment, which are also present in the subsurface of Twin Cave (Fig. 4). The presence of carbonate sedimentary units with similar sedimentary character warrants correlation in the subsurface, but the subunits in Unit 2 (Unit 2A versus 2B) could not be confidently correlated between core sites (Fig. 4). Perhaps the subtle textural variability between Unit 2A and Unit 2B is related to site-specific depositional processes in the conduit from local hydrodynamics or entirely stochastic processes. In HITW Cave, the carbonate sediment pass into the organic deposits at ~5500 cal yr. BP, which suggests a marked change in environmental processes operating the cave. There are no shallower conduit levels in HITW Cave, which suggests that sedimentary processes deeper in the aquifer abruptly changed from conditions promoting carbonate dissolution to a régime dominated by allochthonous organic matter sedimentation.

In Twin Cave, however, sedimentation alternated between the carbonate sediment and organic matter (e.g., TWIN-C1, Fig. 4), which suggests an oscillation of environmental processes (carbonate dissolution vs. allochthonous organic matter supply). This is likely a combination of conduit geometry and elevation. Most cores from Twin Cave are from a shallower conduit level than HITW Cave, and therefore the cores are documenting activity at a shallower level in the aquifer. The vertical chimneys between the upper and lower conduit levels can also permit re-mobilization of sediment from the upper conduit levels to the lower conduit levels. However, the organic matter deposits are temporally constrained with radiocarbon dates, so the prominent organic matter deposits are correlated in the subsurface.

Based on the radiocarbon results (Table 3), the organic matter deposits were emplaced during two pulses that we term Organic Matter Pulse 1 and 2. Organic Matter Pulse 1 (OMP-1) occurred from 13,900 to 12,700 cal yr. BP, which deposited organic matter in both the upper and lower conduit level in Twin Cave. Unit 1 accumulated in the lower conduit levels at TWIN-C1 from 13,950 ± 160 to 13,930 ± 190 cal yr. BP, but was deposited for a longer period of time until 12,762 ± 80 cal yr. BP at the shallower conduit levels (date from TWIN-C4 at 26 to 58 cm). Above OMP-1 in TWIN-C4 is a layer of carbonate sediments, similar to TWIN-C1 from 22 to 65 cm, in TWIN-C4 from 26 to 58 cm, in TWIN-C6 from 21 to 40 cm, and in TWIN-C2 from 38 to 48 cm. Therefore, we correlate this lower organic matter deposit in the subsurface of the Twin Cave cores, but recognize that uncertainty in this correlation remains until further radiocarbon dating is obtained. No Unit 1 accumulated at the TWIN-C5 sampling location, but given the vertical conduit ('vertical chimney') connecting the upper and lower horizontal conduit levels before the TWIN-C5 core site, it is likely that sediment bypassed the site of TWIN-C5 by instead becoming transported down the Skiles Passage or a vertical chimney ('sediment bypass', Fig. 3). If correct, this would indicate that conduit morphology is an important control on sedimentation in inland flooded caves (Fig. 3), which has also been documented for coastal phreatic caves (Collins et al., 2015a).

Organic Matter Pulse-2 (OMP-2) occurred from ~5600 to 3500 cal yr. BP, and is present in both Twin and HITW Cave. A thin deposit of Unit 1 occurs at the top of TWIN-C1 (0–5 cm), with constraining ages at 0 to 1 cm and 4.5 to 5.5 cm of 5170 ± 130 and 3920 ± 50 cal yr. BP, respectively. This age inversion may be related to local bioturbation (e.g., catfish), or erosion of sediment from the upper conduit level, re-mobilization down the vertical chimney, and re-deposition at the lower conduit level. However, the inverted ages still indicate that organic matter influxed into Twin Cave occurred during a discrete time window, though it has since experienced re-mobilization. Closer to the cave exit, the dated twig from Unit 1 in TWIN-C3 at 32.5 cm was aged to 8300 ± 100 cal yr. BP, suggesting that deposition of Unit 1 at this core site was dependent upon its proximal location to the karst window (Fig. 3B). OMP-2 is more expanded in HITW Cave, with a 35-to 75-cm-thick deposit at the tops of all cores from HITW Cave. Based on the radiocarbon results from HITW-C1 (35–36 cm) and in HITW-C2 (34–35 cm), Unit 1 began deposition at 5630 ± 30 and 5530 ± 60 cal yr. BP, respectively (Table 2). Most importantly, these results promote three inferences: (1) that modern sedimentation is negligible in the distal conduits of both caves, (2) that OMP-2 occurred over ~2100 years from 5600 to 3500 cal yr. BP, and (3) OMP-2 deposited more sediment into HITW Cave than Twin Cave.

6. Discussion

6.1. Emplacement of ferromanganese deposits

Iron and manganese oxides and oxyhydroxide minerals dominate the basal sediments recovered from HITW Cave (Units 3–5), which can be more generally referred to as ferromanganese deposits (Ghiorse and Ehlich, 1992; Splide et al., 2006; Gázquez et al., 2011). Thinner horizons of ferromagnesian deposits are also intercalated in Unit 5 at the tops of cores from Twin Cave. However, deposition of these upper Unit 5 horizons likely occurred under different

Table 3
Radiocarbon results on core samples from Hole in the Wall Cave and Twin Cave.

Core	Sampled depth (cm)	Material dated	Conventional ^{14}C age (BP)	δ^{13}C (‰)	2σ calendar ages in yr. BP (probability)	1σ calendar ages in yr. BP (probability)	Calibrated 2σ age (yr BP)
HITW-C1	36 to 37	Bulk organics	4920 ± 30	−29.1	5596–5666 (0.836) 5671–5714 (0.164)	5605–5655 (1)	5630 ± 30
HITW-C2	0–1	Bulk organics	3320 ± 30	−29.7	3470–3625 (1)	3486–3536 (0.547) 3549–3585 (0.453)	3550 ± 75
HITW-C2	34 to 35	Bulk organics	4780 ± 30	−29.15	5468–5590 (1)	5479–5536 (0.871) 5577–5585 (0.129)	5530 ± 60
TWIN-C1	4.5–5.5	Bulk organics	3560 ± 25	−28.39	3728–3748 (0.042) 3764–3792 (0.066) 3823–3926 (0.879) 3949–3959 (0.012)	3834–3889 (1)	3920 ± 50
TWIN-C1	0–1	Bulk organics	4490 ± 30	−28.2	5038–5297 (1)	5052–5077 (0.152) 5104–5134 (0.182) 5162–5195 (0.204) 5206–5280 (0.463)	5170 ± 130
TWIN-C1	23–24	Bulk organics	12,100 ± 45	−31.37	13,787–14,105 (1)	13,853–13,912 (0.288) 13,921–14,045 (0.712)	13,950 ± 160
TWIN-C1	66.5–67.5	Bulk organics	12,000 ± 50	−29.49	13,738–14,013 (1)	13,764–13,872 (0.730) 13,878–13,927 (0.270)	13,930 ± 190
TWIN-C3	32–33	Twig	7500 ± 60	N/M	8198–8393 (1)	8215–8243 (0.189) 8253–8255 (0.013) 8303–8382 (0.798)	8300 ± 100
TWIN-C4	30–31	Bulk organics	10,900 ± 80	N/M	12,689–12,836 (1)	12,704–12,836 (1)	12,760 ± 80
TWIN-C4	55–56	Bulk organics	11,900 ± 80	N/M	13,549–13,978(1)	13,586–13,783 (1)	13,760 ± 220

environmental conditions than the basal ferromagnesian deposits in HITW Cave based on the radiocarbon results (discussed further below), sediment texture and mineralogy (see Section 4.5).

The oxidation of Mn(II) and Fe(II) into solid oxide precipitates can occur inorganically, when the oxygen content or pH of water is increased and enables the precipitation of metal oxides. In caves, a redox gradient can naturally develop across the aquifer-cave boundary as anoxic aquifer waters rich in Mn(II) and Fe(II) ions drain into oxygenated cave systems and forms insoluble Fe(III) and Mn(III, IV) precipitates (de Vitre and Davison, 1993; Martin, 2005; Frierdich and Catalano, 2012; Brown et al., 2014). As such, it has been suggested that thick successions of ferromanganese deposits in Cova des Pas de Vallgornera, Mallorca, were produced inorganically from the oxidization of upwelling (hypogene) groundwater (Fornós et al., 2014).

However, ferromanganese deposits can also be biologically precipitated by Fe- and Mn-oxidizing bacteria (e.g., *Leptothrix*, *Sphaerotilus*, *Clonothrix*, *Thiotrix*, *Hyphomicrobumn*) in oxygenated waters with a near-neutral pH (Peck, 1986). Microbes living in caves can even produce expansive ferromanganese stromatolites (Rossi et al., 2010; Lazano and Rossi, 2012). Biogenic ferromanganese crusts have been identified on cave surfaces, where Mn and Fe are derived from the chemical weathering of the host bedrock (Northup et al., 2003; Spilde et al., 2006; Carmichael et al., 2013). Ferromanganese deposits can also form in freshwater streams flowing through caves and produce ferromanganese crusts (White et al., 2009), shallow sedimentary deposits (Onac et al., 1997; Manolache and Onac, 2000), or pebbles and coatings on pebbles (Frierdich and Catalano, 2012).

In an important example from Florida, Florea et al. (2011) describe the active flocculation and precipitation of iron oxides in Thornton's Cave by *Leptothrix* (Withlacoochee River drainage basin; Fig. 1). Depending on the season, Thornton's Cave functions as either a sink (siphon) or spring (estavelle) with the adjacent Withlacoochee River (Fig. 1). The local water table is positioned within the conduits of Thornton's Cave, and the elevation of the water table oscillates with the seasons (Florea et al., 2011). If we assume that the overall stratigraphic architecture in HITW Cave is organized from oldest to youngest, then a minimum age for the basal ferromanganese deposits is the late Pleistocene, and the basal deposits would likely be coincident with periods of lower aquifer water levels during lower eustatic sea levels (Florea et al., 2007). It is possible that Thornton's Cave provides a modern analog for paleo environmental conditions when the ferromanganese deposits were emplaced in HITW and Twin Cave. No evidence of desiccation or induration was observed in our cores, such as has been observed in Mallorcan cave sediments (Fornós et al., 2009), which suggests continuously humid conditions or intermittent standing water in the cave. Additional modern sedimentary analogs are required to better understand environmental conditions in the cave during deposition of the ferromanganese deposits.

At this stage, it is uncertain whether inorganic or biologic processes drove precipitation of the ferromanganese deposits, or specifically how these processes relate to the paleo water table (vadose zone, phreatic zone, or at the water table). The presence of coarse-grained fossil horizons does suggest some occasional increased water flow and/or calcite dissolution. However, the preservation of fine laminations throughout Units 3–5 indicates that quiescent water conditions were dominant. Lower eustatic sea level during the late Pleistocene likely placed the local water table considerably closer to, or below, the basal conduit level of HITW Cave (Florea et al., 2007), which certainly altered regional hydrogeology. At this stage, it would be speculative to provide a specific elevation of the paleo table during the Pleistocene, as the water table elevation inland is complex. However, such prehistoric water levels perhaps generated a hydrographic system in HITW Cave that is partially analogous to modern conditions in Thornton's Cave. Such a scenario would also explain the absence of thick ferromanganese deposits in the horizontal conduits at a shallower level in the subsurface in Twin Cave (Fig. 3B), which may have been completely in the vadose zone during contemporaneous deposition of Units 3 and 4 in HITW Cave. Alternatively, the absence of thick ferromanganese deposits in Twin Cave at the shallower conduit levels may give credibility to a hypogene source of trace metals for deposition in HITW Cave, since Twin Cave would have provided a thoroughfare of terrestrially sourced water (epigene) to the paleo water table of the Upper Floridian Aquifer. Further geochemical research is required to determine the origin and emplacement history of the ferromanganese deposits.

6.2. Enhanced limestone dissolution and carbonate sedimentation

Deposition of carbonate sediment (Unit 2) in both caves likely indicates similar environmental conditions. Unfortunately, the timing for

the emplacement of the carbonate sediment is poorly understood because of a lack of suitable material for radiocarbon dating. However, the radiocarbon ages at the contact with Unit 1 in both Twin Cave (TWIN-C4) and in HITW Cave (HITW-C1,C2) indicate emplacement at least from the early to middle Holocene, and the core logs indicate that deposition typically occurs *after* accumulation of the ferromanganese deposits (Fig. 4). It is striking that carbonate sedimentation in HITW Cave terminated in the mid-Holocene. This suggests that the conditions required for enhanced carbonate dissolution are not constant in geologic time or geographic space, but they are likely linked to specific paleoenvironmental conditions.

Based on the abundance of marine invertebrate fossil remains (e.g., shark teeth, echinoid spines), these sediments likely evidence periods of enhanced bedrock dissolution and conduit expansion during lower paleo water tables. Florea et al. (2007) noted the prevalence of cave passages in west-central Florida at 12–15 m above modern sea level and 35 m below the modern water table, and suggested their prevalence was associated with enhanced dissolution at specific paleo water tables during previous sea-level lowstands. Recently, Gulley et al. (2015) describe how heterogeneous pCO_2 concentrations in freshwater meteoric lenses is likely contributing to dissolution of Florida's caves, a process that is amplified when terrestrial water flows into a subsurface cave (Gulley et al., 2011). In the modern environment, Brown et al. (2014) documented enhanced calcite dissolution and ferromanganese deposition in Madison Blue Cave System (Suwanee River drainage basin) caused by river reversals during storms. Madison Blue usually functions as a spring and discharges water into the Santa Fe River, but intense precipitation causes river water to instead to flush into the cave (siphon) and push groundwater into the aquifer matrix porosity, which promotes calcite dissolution and trace metal sorption from the bedrock. As storm levels recede, reduced water from the aquifer matrix porosity re-enters conduits with oxygenated cave water to precipitate metal oxides on cave walls. However, Gulley et al. (2013) suggested that river reversals alone have not generated Florida's phreatic caves as there would be little way to force floodwater below a water table level without a pre-existing void. Given the large successions of pre-Holocene carbonate sedimentation in HITW and Twin Caves, the suggestion of Gulley et al. (2013) seems valid. In fact, the carbonate sedimentation concurs with the hypothesis of Gulley et al. (2013) and Florea et al. (2007) that enhanced dissolution most likely occurs at paleo water tables. However, stratigraphic analysis of sediments emplaced in phreatic caves in eastern Florida is needed to further evaluate this hypothesis.

6.3. Organic matter deposition and linkage to the Apalachicola River drainage basin

Deposition of Unit 1 appears closely linked to known intervals of climate change and activation of surficial hydrologic networks in the Floridian region. Cave systems in the Upper Floridian Aquifer are an integral part of the regional hydrologic cycle, such that one would predict that precipitation variability and base level changes caused by glacioeustatic sea levels could influence the environments in subsurface void spaces (Florea et al., 2007; Gulley et al., 2013).

The deposition of Organic Matter Pulse 1 (OMP-1) in Twin Cave from 13,900 to 12,700 cal yr. BP coincides with the Bølling/Allerød climate oscillation, which is a period of general global climate warming that terminated with a return to cold, glacial-like climate conditions at the onset of the Younger Dryas at ~12,700 yr. BP (Bard et al., 2010; Deschamps et al., 2012) (Fig. 8). The lack of OMP-1 in HITW Cave suggests that either (a) the HITW karst window was not yet open, or (b) the surficial stream in Merritt's Mill Pond that was transporting organics into Twin Cave was not interacting with the karst window on the side of the stream channel that is the entrance to HITW Cave. Based on pollen reconstructions from Camel Lake (Watts et al., 1992) and Sheelar Lake (Watts, 1980), northern Florida was dominated by mesic, temperate forests through the Bølling/Allerød Interstadial, which would indicate that the precipitation was high (Overpeck et al., 1989) (Figs. 1, 8). However, spruce populations near Camel Lake from 14,330 ± 275 cal yr. BP to 12,610 ± 135 cal yr. BP indicate that the lower Apalachicola River drainage basin was unusually cool at this time (Watts et al., 1992), thus behaving paradoxically to the global trend towards warmer environments during this period. It is possible that regional cooling of Northwestern Florida during the Bølling/Allerød Interstadial is related to the cooling of the Gulf of Mexico caused by Mississippi River discharge of glacial meltwater between 14,650 and 13,600 yr. BP (Fairbanks, 1989; Bard et al., 1990; Deschamps et al., 2012) (Fig. 8), which is thought to have also rapidly changed sea level by as little as 0.66 ± 0.07 m (Wickert et al., 2013) or as much as 17 ± 5 m (Deschamps et al., 2012). This sea-level rise could have had a significant effect on the water table level and hydrodynamics of the Upper Floridian Aquifer in northwestern Florida, perhaps even promoting short-lived surface streams and ponds. Such changes in surface and groundwater hydrology could be related to deposition of OMP-1.

After deposition of OMP-1 in Twin Cave, carbonate sedimentation resumes at the upper horizontal conduit level, whereas Unit 5 (ferromanganese-rich sandy carbonate mud) is deposited in the lower conduit level (TWIN-C1, Fig. 3). In nearby Camel Lake, a depositional

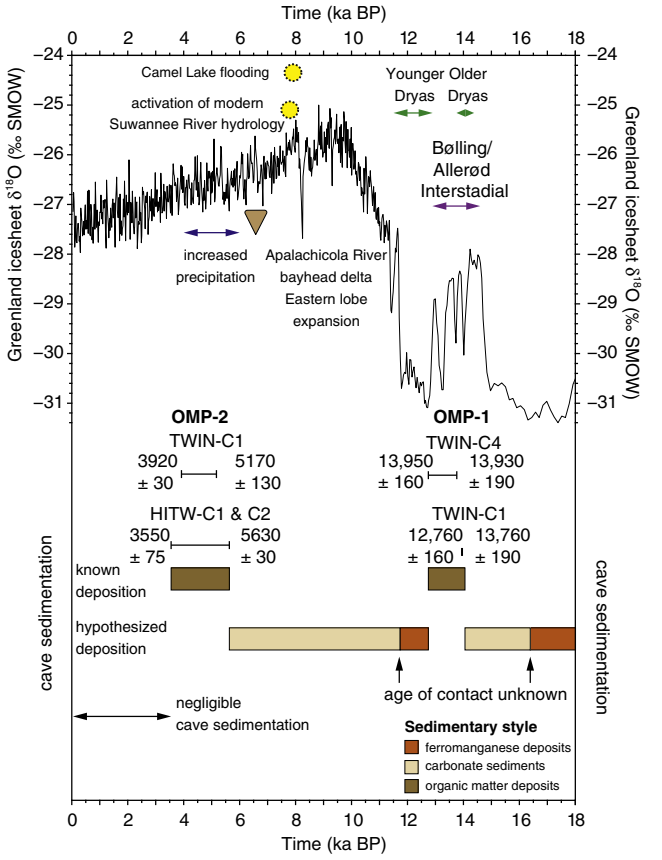

Fig. 8. Comparison of cave sedimentation to global climate variability over the last 20,000 years. $\delta^{18}O$ isotopic curve from Greenland Ice Cores in Eastern Greenland (Vinther et al., 2008) and important global climate events (Fairbanks, 1989; Deschamps et al., 2012). Initiation of modern surficial hydrographic networks in Florida is indicated by flooding of Camel Lake by water table rise (Watts et al., 1992), extension of the eastern lobe of the Apalachicola River bayhead delta (Osterman et al., 2009), increase in regional precipitation at ~5000 yr. BP based on Sheelar Lake, Goshen Springs, and Little Salt Spring (Delcourt, 1980; Watts and Stuiver, 1980; Watts and Hansen, 1988; Alverez Zarikian et al., 2005), and potential activation of surficial hydrology in the Suwaneee River drainage basin (Gulley et al., 2013) at ~7900 cal yr. BP (Milliken et al., 2008). Stratigraphic emplacement of the three primary depositional styles in Hole in the Wall Cave (HITW) and Twin Cave is based on available radiocarbon dates and general and stratigraphic architecture.

hiatus occurred from ~10,000 to 7000 yr. BP (Figs. 1, 8). It is thought that this depositional hiatus is related to lowering of the Upper Floridian Aquifer or significant regional aridity (Watts et al., 1992). If this interpretation is correct, then carbonate sediment from enhanced bedrock dissolution resumed in the upper conduit levels in Twin Cave.

Deposition of OMP-2 from 5600 to 3600 cal yr. BP likely occurred after the Upper Floridian Aquifer flooded and activated modern surficial hydrographic features (lakes, streams), and is correlated with increased regional precipitation and discharge through the Apalachicola River drainage basin (Figs. 1, 8). Given the antecedent carbonate bedrock, it has been suggested that many surficial hydrologic networks (i.e., lakes, streams) in Florida were initiated as early as ~8000 yr. BP, as Holocene sea-level rise forced vertical migration of the Upper Floridian Aquifer into regional topographic lows (Watts and Hansen, 1988; Gulley et al., 2014). For example, the Suwannee River only incised a valley to ~9 m below sea level in the Gulf of Mexico (Wright et al., 2005), suggesting that Holocene drainage through the Suwannee River only initiated after topographic lows on the Ocala Karst Plain were inundated by sea level-forced vertical migration Upper Floridian Aquifer (Fig. 1). In the Apalachicola River drainage basin, perhaps Merritt's Mill Pond was a dry basin until ~6000 yr. BP, but inundation by the Upper Floridian Aquifer thereafter activated the surficial stream network and initiated erosion of terrestrial organic matter into HITW Cave and Twin Cave. At the coastline in Apalachicola Bay, estuarine conditions were initiated at ~6400 yr. BP (Fig. 8) when sea level in the Gulf of Mexico was ~6 m below present (Milliken et al., 2008). More specifically, an eastern lobe of the modern Apalachicola River bayhead delta was only active from 5800 to 5100 yr. BP (Osterman et al., 2009; Twichell et al., 2010) during a known increase in regional precipitation. In a review of Floridian lake level history, Watts and Hansen (1988) suggest increased swamping in northern Florida from 5000 to 2500 yr. BP was related to increased regional precipitation (Fig. 8). Similarly, a pollen reconstruction from Goshen Springs in southern Alabama (Fig. 1) also indicates increased precipitation beginning at ~5000 yr. BP (Delcourt, 1980). In Southern Florida, $\delta^{18}O$ ratios from ostracodes living in Little Salt Spring document increased rainfall from ~5700 to 4000 yr. BP (Alverez Zarikian et al., 2005). Collectively, these records suggest that deposition of OMP-1 occurred after the Upper Floridian Aquifer flooded topographic lows and initiated drainage through the Apalachicola River drainage basin; but also coincides with evidence for invigorated flow through the Apalachicola River drainage basin related to increased regional precipitation.

In the topmost portion of the cores, "yellowish red" (5YR 4/6) ferromanganese mineralization is present that is either (a) a narrow deposit in HITW Cave, or (b) part of Unit 5 in Twin Cave (Figs. 4-6). Given that these sediments are likely deposited after regional base-level rise decelerated in the middle Holocene, it seems likely that the seasonal geochemical processes described at Madison Blue in the Suwanee River drainage basin by Brown et al. (2014) are also operating at Twin and HITW Caves. Alternatively, this narrow layer of ferromanganese deposits represents a redox boundary as anoxic hypogene water is oxidized when it encounters the oxygenated conduit.

7. Conclusions

- Late Quaternary detrital sedimentation in two phreatic caves in northwestern Florida appears broadly linked to ocean and atmospheric forcing, whereby feedbacks between sea level and the local water table elevation and regional precipitation patterns impact cave sedimentation.
- Six distinct facies were identified in the subsurface of HITW Cave and Twin Cave in Marianna, Florida, USA, which can be grouped into three broad sedimentary styles that are related to base-level variability of the Upper Floridian Aquifer throughout the Late Quaternary. The general architecture of these primary sedimentary styles in a transgressive sequence, from bottom to top is: *ferromanganese deposits, carbonate sediment,* and *organic matter deposits*. Lateral textural variability was also observed, as sedimentation in conduits closest to the karst window were different than deeper into the cave.
- Ferromanganese deposits were likely deposited during lower base levels of the Upper Floridian Aquifer during the late Pleistocene. It remains uncertain if they are derived from biologic (e.g., bacterial) or inorganic (e.g., oxidation of hypogene waters) processes.
- Texturally variable carbonate sediment that is generally Ca- and Sr-rich, and Mn- and Fe-poor was also likely deposited during lower paleo water levels. The abundance of invertebrate fossils within these sediments suggests that they document periods of enhanced limestone dissolution. Based on the successions from lower conduit levels in HITW Cave, the environmental conditions necessary for enhanced dissolution and carbonate sedimentation have not occurred over the last 5600 years. However, the environmental conditions necessary for enhanced dissolution may have persisted at the shallower conduit levels of TWIN Cave until more recently (Fig. 3).
- Organic matter deposits accumulate proximal to the cave exits (karst windows), and their pulsed deposition occurred during discrete time intervals, perhaps evidencing when invigorated flow occurred through the Apalachicola River drainage basin. For example, OMP-1 (~14,000 cal yr. BP) occurred during the Bølling/Allerød climate oscillation, and OMP-2 (5600 to 3600 cal yr. BP) occurred during an interval of increased regional precipitation in the southern USA.
- Analysis of successions from other Floridian caves is required to assess the regional continuity of these sedimentary signals, their climatic forcing, and further refine their emplacement history.

Acknowledgements

Field support was provided by M. Loyco, E. Sorenson and the staff at *Cave Adventures*, and technical support was provided by K. Schwehr. Funding for this project was provided by The Explorer's Club Youth Activity Fund, Society for Sedimentary Geology, Texas Institute of Oceanography, the Geological Society of America, and NSF Award OCE-1356509.

A. Supplementary data

Supplementary data associated with this article can be found in the online version, at http://dx.doi.org/10.1016/j.sedgeo.2016.01.022. These data include the Google maps of the most important areas described in this article.

References

Alverez Zarikian, C.A., Swart, P.K., Gifford, J.A., Blackwelder, P.L., 2005. Holocene paleohydrology of Little Salt Spring, Florida, based on ostracod assemblages and stable isotopes. Palaeogeography, Palaeoclimatology, Palaeoecology 225, 134–156.

Anderson, J.B., Rodriguez, A.B., Milliken, K., Taviani, M., 2008. The Holocene evolution of the Galveston estuary complex, Texas: evidence for rapid change in estuarine environments. Geological Society of America Special Papers 443, 89–104.

Bard, E., Hamelin, B., Fairbanks, R.G., 1990. U-Th ages obtained by mass spectrometry in corals from Barbados: sea level during the past 130, 000 years. Nature 346, 456–458.

Bard, E., Hamelin, B., Delanghe-Sabatier, D., 2010. Deglacial meltwater pulse 1B and Younger Dryas sea levels revisted with boreholes at Tahiti. Science 327, 1235–1237.

Bates, A.L., Spiker, E.C., Hatcher, P.G., Stout, S.A., Weintraub, V.C., 1995. Sulfer geochemistry of organic rich sediments from Mud Lake, Florida, USA. Chemical Geology 121, 245–262.

Bosch, R.F., White, B., 2007. Lithofacies and Transport of Clastic Sediments in Karstic Aquifers. In: Sasowsky, I.D., Mylroie, J. (Eds.), Studies of Cave Sediments: Physical and Chemical Records of Paleoclimate. Springer US, New York City, NY, pp. 1–22.

Boyle, J., 2004. Comment: A comparison of two methods for estimating the organic matter content of sediments. Journal of Paleolimnology 31, 125–127.

Brandon, C., Woodruff, J.D., Lane, P., Donnelly, J.P., 2013. Constraining flooding conditions for prehistoric hurricanes from resultant deposits preserved in Florida sinkholes. Geochemistry, Geophysics, Geosystems 14, 2993–3008.

Brinkmann, R., Reeder, P.P., 1994. The influence of sea-level change and geologic structure on cave development in West-Central Florida. Physical Geography 15, 52–61.

Brown, A.L., Martin, J.B., Screaton, E.J., Ezell, J.E., Spellman, P., Gulley, J., 2014. Bank storage in karst aquifers: the impact of temporary intrusion of river water on carbonate dissolution and trace metal mobility. Chemical Geology 385, 56–69.

Carmichael, S.K., Carmichael, M.J., Strom, A., Johnson, K.W., Roble, L.A., Gao, Y., BRA, S.L., 2013. Sustained anthropogenic impact in Carter Saltpeter Cave, Carter County, Tennessee and the potential effects On manganese cycling. Journal of Cave and Karst Studies 75, 189.
Chen, C.S., 1965. The Regional Lithostatigraphic Analysis of Paleocene and Eocene Rocks of Florida.
Collins, S.V., Reinhardt, E.G., Rissolo, D., Chatters, J.C., Nava Blank, A., Luna Erreguerena, P., 2015a. Reconstructing water level in Hoyo Negro, Quintana Roo, Mexico, implications for early Paleoamerican and faunal access. Quaternary Science Reviews 438, 124–134.
Collins, S.V., Reinhardt, E.G., Werner, C.L., Le Maillot, C., Devos, F., Rissolo, D., 2015b. Late Holocene mangrove development and onset of sedimentation in the Yax Chen cave system (Ox Bel Ha) Yucatan Mexico: implications for using cave sediments as a sea-level indicator. Palaeogeography, Palaeoclimatology, Palaeoecology 438, 124–134.
Cooke, C.W., 1939. Scenery of Florida Interpreted by a Geologist. Bulletin 17. Florida Geological Survey, Tallahassee, FL.
Cooke, C.W., 1945. Geology of Florida. Bulletin 37. The Florida Geological Survey, Tallahassee, FL.
Davison, W., 1993. Iron and manganese in lakes. Earth-Science Reviews 34, 119–163.
de Vitre, R., Davison, W., 1993. Manganese Particles in Freshwater. In: Buffle, J., van Leeuwin, H.P. (Eds.), Environmental Particles. Lewis Publishers, Boca Raton, FL, pp. 317–352.
Dean, W.E., 1974. Loss on ignition as a method for estimating organic and carbonate content in sediments: reproducibility and comparability of results. Journal of Paleolimnology 25, 101–110.
Delcourt, P.A., 1980. Goshen Springs: Late Quaternary vegetation record for Southern Alabama. Ecology 371-386.
Denomee, K.C., Bentley, S.J., Droxler, A.W., 2014. Climatic control on hurricane patterns: a 1200-y near-annual record from Lighthouse Reef, Belize. Scientific Reports 4, 7.
Deschamps, P., Durand, N., Bard, E., Hamelin, B., Camoin, G., Thomas, A.L., Henderson, G.M., Okuna, J., Yokoyama, Y., 2012. Ice-sheet collapse and sea-level rise at the Bølling warming 14,600 years ago. Nature 483, 559–564.
Dodson, J., 2013. Final Report Nutrient TMDL for Jackson Blue Spring and Merritts Mill Pond (WBIDs 180Z and 180A). Florida Department of Environmental Protection, Division of Environmental Assessment and Restoration, Bureau of Watershed Restoration, Northwest District-Apalachicola-Chipola Basin, Tallahassee.
Dufresne, D.P., Drake, D.R., 1999. Regional groundwater flow model construction and wellfield site selection in a karst area, Lake City, Florida. Engineering Geology 52, 129–139.
Fairbanks, R.G., 1989. A 17,000-year glacio-eustatic sea level record: influence of glacial melting rates on the Younger Dryas even and deep-ocean circulation. Nature 342, 637–642.
Fawcett, T., Faber, J., Kabbekodu, S., McClune, F., Rafaja, D., 2005. PDF-4+ 2005 (Database), Microstructure Analysis in Materials Science. International Centre for Diffraction Data, Newtown Square, PA, USA.
Filley, T.R., Freeman, K.H., Bianchi, T.S., Colarusso, L.A., Hatcher, P.G., 2001. An isotopic biogeochemical assessment of shifts in organic matter input to Holocene sediments from Mud Lake, Florida. Organic Geochemistry 32, 1153–1167.
Florea, L.J., Vacher, H.L., Donahue, B., Naar, D., 2007. Quaternary cave levels in peninsular Florida. Quaternary Science Reviews 26, 1344–1361.
Florea, L.J., Stinson, C.L., Brewer, J., Fowler, R., Kearns, B.J., Greco, A.M., 2011. Iron oxide and calcite associated with *Leptothrix* sp. biofilms within an estavelle in the Upper Floridian Aquifer. International Journal of Speleology 40, 205–219.
Ford, D., Williams, P., 1989. Karst Geomorphology and Hydrology. Unwin Hyman, London.
Fornós, J.J., Ginés, J., Gràcia, F., 2009. Present-day sedimentary facies in the coastal karst caves of Mallorca Island (Western Mediterranean). Journal of Cave and Karst Studies 71, 86–99.
Fornós, J., Ginés, A., Gracia, F., Merino, A., Gomez-Pujol, L., Bover, P., 2014. Cave deposits and sedimentary processes in Cova des Pas de Vallgornera (Mallorca, Western Mediterranean). International Journal of Speleology 43, 159–175.
Frierdich, A.J., Catalano, J.G., 2012. Distribution and speciation of trace elements in iron and manganese oxide cave deposits. Geochimica et Cosmochimica Acta 91, 240–253.
Frydenbourg, R., 2006. Water Quality Study of the Ichetucknee River. Florida Department Of Environmental Protection, Tallahassee, FL.
Gabriel, J.J., 2009. Late Holocene (3500 yBP) Salinity Changes and their Climatic Implications as Recorded in an Anchialine Cave System, Ox Bel Ha, Yucatan, Mexico MSc Thesis McMaster University (95 pp).
Gascoyne, M., Benjamin, G.J., Schwarcz, H.P., Ford, D.C., 1979. Sea-level lowering during the Illinoian Glaciation: evidence from a Bahama "Blue Hole". Science 205, 806–808.
Gázquez, F., Calaforra, J.M., Forti, P., 2011. Black Mn-Fe crusts as markers of abrupt paleoenvironmental changes in El Soplao Cave (Canabria, Spain). International Journal of Speleology 40, 163–169.
Ghiorse, W.C., Ehlich, H.I., 1992. Microbial biomineralization of iron and manganese. Catena Supplement 21, 75–99.
Green, R.C., Williams, C.P., Paul, D.T., Kromhout, C., Scott, T.M., 2009. Geomorphology, springs, and karst features of the eastern portion of the USGS Ocala 30 X 60 minute quadrangle, North-Central Florida, Open-File Map. Florida Geological Survey (pp. Plate 3).
Grimm, E.C., Jacobson, G.L., Watts, W.A., Hansen, B.C.S., Maasch, K.A., 1993. A 50,000-year record of climate oscillations from Florida and its temporal correlation with the Heinrich events. Science 261, 198–200.
Gulley, J.D., Martin, J.B., Screaton, E.J., Moore, P.J., 2011. River reversals into karst springs: a model for cave enlargement in eogenetic karst aquifers. Geological Society of America Bulletin 123, 457–467.
Gulley, J.D., Martin, J.B., Moore, P.J., Murphy, J., 2013. Formation of phreatic caves in an eogenetic karst aquifer by CO_2 enrichment at lower water tables and subsequent flooding by sea level rise. Earth Surface Processes and Landforms 38, 1210–1224.
Gulley, J., Martin, J., Spellman, P., Moore, P., Screaton, E., 2014. Influence of partial confinement and Holocene river formation on groundwater flow and dissolution in the Florida carbonate platform. Hydrological Processes 28, 705–717.
Gulley, J.D., Martin, J.B., Moore, P.J., Brown, A., Spellman, P.D., Ezell, J., 2015. Heterogeneous distributions of CO_2 may be more important for dissolution and karstification in coastal eogenetic limestone than mixing dissolution. Earth Surface Processes and Landforms 40, 1057–1071.
Heiri, O., Lotter, A.F., Lemcke, G., 2001. Loss on ignition as a method for estimating organic and carbonate content in sediments: reproducibility and comparability of results. Journal of Paleolimnology 25, 101–110.
Hill, C.A., 1982. Origin of black deposits in caves. National Speleological Society Bulletin 44, 15–19.
Jin, J., Zimmerman, A.R., Moore, P.J., Martin, J.B., 2014. Organic and inorganic carbon dynamics in a karst aquifer: Sante Fe River sink-rise system. Journal of Geophysical Research, Biogeosciences 119, 340–357.
Keating, B., 1985. Submersible Observations on the Flanks of Johnston Island (Central Pacific Ocean). Proceedings of the Fifth International Coral Reef Congress, Tahiti, pp. 413–418.
Kurz, M.J., Martin, J.B., Cohen, M.J., Hensley, R.T., 2015. Diffusion and seepage-driven element fluxes from the hyporheic zone of a karst river. Freshwater Science 34, 206–221.
Lane, P., Donnelly, J.P., Woodruff, J.D., Hawkes, A.D., 2011. A decadally-resolved paleohurricane record archived in the late Holocene sediments of a Florida sinkhole. Marine Geology 287, 14–30.
Larsen, E., Mangerud, J., 1989. Marine caves: on–off signals for glaciations. Quaternary International 3 (4), 13–19.
Lazano, R.P., Rossi, C., 2012. Exceptional preservation of Mn-oxidizing microbes in cave stromatolies (El Soplao, Spain). Sedimentary Geology 255-256, 42–55.
Lehner, B., Grill, G., 2013. Global river hydrography and network routing: baseline data and new approaches to study the world's large river systems. Hydrological Processes 27, 2171–2186.
Lind, C., Hem, J., Roberson, C., 1987. Reaction products of manganese-bearing waters. Chemical Quality of Water and the Hydrological Cycle, pp. 273–301.
Manolache, E., Onac, B.P., 2000. Geomicrobiology of black sediments in Vantului Cave (Romania): preliminary results. Cave and Karst Science 27 pp. 109–112.
Martin, S.T., 2005. Precipitation and dissolution of iron and manganese oxides. Environmental Catalysis, pp. 61–81.
Martin, J.B., Dean, R.W., 2001. Exchange of water between conduits and matrix in the Floridian aquifer. Chemical Geology 179, 145–165.
Martin, H.W., Harris, W.G., 1992. Mineralogy of clay sediments in three phreatic aves of the Suwanee River Basin. National Speleological Society Bulletin 54, 69–76.
Milliken, K., Anderson, J.B., Rodriguez, A.B., 2008. A new composite Holocene sea-level curve for the Northern Gulf of Mexico. Geological Society of America Special Papers 443, 1–11.
Moore, W., 1955. Geology of Jackson County, Florida.
Northup, D.E., Barns, S.M., Yu, L.E., Spilde, M.N., Schelble, R.T., Dano, K.E., Crossey, L.J., Connolly, C.A., Boston, P.J., Natvig, D.O., 2003. Diverse microbial communities inhabiting ferromanganese deposits in Lechuguilla and Spider Caves. Environmental Microbiology 5, 1071–1086.
Onac, B.P., Pedersen, R.B., Tysseland, M., 1997. Presence of rare-earth elements in black ferromanganese coatings from Vântului Cave (Romania). Journal of Caves and Karst Studies 59, 128–131.
Onac, B.P., Fornós, J., Merino, A., Ginés, J., Diehl, J., 2014. Linking mineral deposits to speleogenetic processes in Cova des Pas de Vallgornera (Mallorca, Spain). International Journal of Speleology 43, 4.
Onac, B.P., Hutchinson, S.M., Geanta, A., Forray, F.L., Wynn, J.G., Giurgiu, A.M., Coroiu, I., 2015. A 2500-yr late Holocene multi-proxy record of vegetation and hydrologic changes from a cave guano-clay sequence in SW Romania. Quaternary Research 83, 437–448.
Osterman, L., Twichell, D.C., Poore, R., 2009. Holocene evolution of Apalachicola Bay, Florida. Geo-Marine Letters 29, 395–404.
Overpeck, J.T., Peterson, L.C., Kipp, N., Imbrie, J., Rind, D., 1989. Climate change in the circum-North Atlantic region during the last deglaciation. Nature 338, 553–557.
Oyen, C.W., Protell, R.W., 2001. Diversity and patterns of biostratigraphy of Cenozoic echinoderms from Florida. Palaeogeography, Palaeoclimatology, Palaeoecology 166, 193–218.
Palmer, A.N., 2007. Cave Geology. Cave Books.
Peck, S.B., 1986. Bacterial deposition of iron and manganese oxides in North American caves. National Speleological Society Bulletin 48, 26–30.
Peltier, W.R., Fairbanks, R.G., 2006. Global glacial ice volume and last glacial maximum duration from an extended Barbados sea level record. Quaternary Science Reviews 25, 3322–3337.
Polk, J.S., van Beynen, P.E., Asmerom, Y., Polyak, V., 2013. Reconstructing past climates using carbon isotopes from fulvic acids in cave sediments. Chemical Geology 360-361, 1–9.
Puri, H., 1964. Stratigraphy and zonation of the Ocala Group: Florida Geological Survey Bulletin 38, (248 p., and Vernon. RO).
Quillen, A.K., Gaiser, E.E., Grimm, E.C., 2013. Diatom-based paleolimnological reconstruction of regional climate and local land-use change from a protected sinkhole lake in Southern Florida, USA. Journal of Paleolimnology 49, 15–30.
Randazzo, A.F., Zachos, L.G., 1984. Classification and description of dolomitic fabrics of rocks from the Floridian aquifer, USA. Sedimentary Geology 37, 151–162.
Randazzo, A.F., Kosters, M., Jones, D.S., Portell, R.W., 1990. Paleoecology of shallow-maine carbonates, middle Eocene of Peninsular Florida. Sedimentary Geology 66, 1–11.
Reimer, P.J., Bard, E., Bayliss, A., Beck, J.W., Blackwell, P.G., Ramsey, C.B., Buck, C.E., Cheng, H., Edwards, R.L., Friedrich, M., 2013. IntCal13 and Marine13 radiocarbon age calibration curves 0–50,000 years cal BP. Radiocarbon 55, 1869–1887.

Rhoades, R., Sinacori, M.N., 1941. Pattern of ground-water flow and solution. Journal of Geology 49, 785–794.
Rossi, C., Lozano, R.P., Isanta, N., Hellstrom, J., 2010. Manganese stromatolites in caves: El Soplao (Cantabria, Spain). Geology 38, 1119–1122.
Rupert, F.R., 1988. The Geology of Wakulla Springs. Open File Report 22. Florida Geological Survey, Tallahassee, FL.
Rupert, F.R., 1991. Lithology and Palynology of Cave Floor Sediment Cores from Wakulla Spring, Wakulla County, Florida. Open Flle Report 47 (Tallahasse, Florida).
Ryan, W.B., Carbotte, S.M., Coplan, J.O., O'Hara, S., Melkonian, A., Arko, R., Weissel, R.A., Ferrini, V., Goodwillie, A., Nitsche, F., 2009. Global multi-resolution topography synthesis. Geochemistry, Geophysics, Geosystems 10.
Schmidt, W., 1988. Florida Caverns State Park, Jackson County, Florida, Open File Report 23. Florida Geological Survey, Tallahassee, FL.
Shinn, E.A., Reich, C.D., Locker, S.D., Hine, A.C., 1996. A giant sediment trap in the Florida Keys. Journal of Coastal Research 12, 953–959.
Spencer, S.M., Lloyd, J.M., 1999. Mineral Resources of Jackson County, Florida (Tallahassee, Florida).
Spilde, M.N., Northup, D.E., Boston, P.J., 2006. Ferromanganese Deposits in the Caves of the Guadalupe Mountains, New Mexico Geological Society 57th Annual Fall Field Conference Guidebook. New Mexico Geological Society, p. 344.
Splide, M.N., Northrup, D.E., Boston, P.J., 2006. Ferromanganese deposits in the caves of the Guadalupe Mountains. In: Land, L., Leuth, V.W., Raatz, W., Boston, P., Love, D.L. (Eds.), New Mexico Geological Society 57th Annual Fall Field Conference Guidebook, pp. 161–165.
Springer, G.S., Kite, J.S., 1997. River derived slackwater sediments in caves along Cheat River, West Virgina. Geomorphology 18, 91–100.
Springer, G.S., Kite, J.S., Schmidt, V.A., 1997. Cave sedimentation, genesis, and erosional history in the Cheat River Canyon, West Virginia. Geological Society of America Bulletin 109 (542–532).
Streever, W.J., 1996. Energy economy hypothesis and the troglobitic crayfish *Procambarus erythrops* in Sim's Sink Cave, Florida. American Midland Naturalist 135, 357–366.
Survey, F.G., Scott, T.M., Anderson, D., 2001. Geologic Map of the State of Florida. Florida Geological Survey.
Teeter, J.W., 1995. Holocene Saline Lake History, San Salvador Island, Bahamas. In: Curan, H.A., White, B. (Eds.), Terrestrial and Shallow Marine Geology of the Bahamas and Bermuda. Geological Society of America Special Paper 300, pp. 117–124.
Teeter, J.W., Quick, T.J., 1990. Magnesium salinity relation in the saline late ostracode *Cyprideis americana*. Geology 18, 220–222.
Twichell, D., Edmiston, L., Andrews, B., Stevenson, W., Donoghue, J., Poore, R., Osterman, L., 2010. Geologic controls on the recent evolution of oyster reefs in Apalachicola Bay and St. George Sound, Florida. Estuarine, Coastal and Shelf Science 88, 385–394.
van Hengstum, P.J., Reinhardt, E.G., Beddows, P.A., Gabriel, J.J., 2010. Investigating linkages between Holocene paleoclimate and paleohydrogeology preserved in a Yucatan underwater cave. Quaternary Science Reviews 29, 2788–2798.
van Hengstum, P.J., Scott, D.B., Gröcke, D.R., Charette, M.A., 2011. Sea level controls sedimentation and environments in coastal caves and sinkholes. Marine Geology 286, 35–50.
van Hengstum, P.J., Donnelly, J.P., Toomey, M.R., Albury, N.A., Lane, P., Kakuk, B., 2014. Heightened hurricane activity on the Little Bahama Bank from 1350 to 1650 AD. Continental Shelf Research 86, 103–115.
van Hengstum, P.J., Donnelly, J.P., Kingston, A.W., Williams, B.E., Scott, D.B., Reinhardt, E.G., Little, S.N., Patterson, W.P., 2015a. Low-frequency storminess signal at Bermuda linked to cooling events in the North Atlantic region. Paleoceanography 30, 52–76.
van Hengstum, P.J., Richards, D.A., Onac, B.P., Dorale, J.A., 2015b. Coastal Caves and Sinkholes. In: Shennan, I., Long, A.J., Horton, B.P. (Eds.), Handbook of Sea-Level Research. John Wiley and Sons.
van Hengstum, P.J., Donnelly, J.P., Fall, P.L., Toomey, M.R., Albury, N.A., Kakuk, B., 2016. The intertropical convergence zone modulates hurricane strikes on the western North Atlantic margin. Scientific Reports 6, 21728.
Vinther, B.M., Clausen, H.B., Fisher, D., Koerner, R., Johnsen, S.J., Andersen, K.K., Dahl-Jensen, D., Rasmussen, S.O., Steffensen, J.P., Svensson, A., 2008. Synchronizing ice cores from the Renland and Agassiz ice caps to the Greenland ice core chronology. Journal of Geophysical Research – Atmospheres 113 (1984–2012).
Watts, W.A., 1969. A pollen diagram from Mud Lake, Marion County, North-Central Florida. Geological Society of America Bulletin 80, 631–642.
Watts, W.A., 1980. The Late Quaternary vegetation history of the southeastern United States. Annual Review of Ecology and Systematics 387–409.
Watts, W.A., Hansen, B.C., 1988. Environments of Florida in the Late Wisconsin and Holocene. Wet Site Archaeology, pp. 307–323.
Watts, W.A., Hansen, B.C.S., 1994. Pre-Holocene and Holocene pollen records of vegetation history from the Florida peninsula and their paleoclimatic implications. Palaeogeography, Palaeoclimatology, Palaeoecology 109, 163–176.
Watts, W.A., Stuiver, M., 1980. Late Wisconsin climate of Northern Florida and the origin of species-rich deciduous forest. Science 210, 325–327.
Watts, W.A., Hansen, B.C.S., Grimm, E.C., 1992. Camel Lake: A 40 000-yr record of vegetational and forest history from Northwest Florida. Ecology 1056-1066.
White, W.A., 1970. The Geomorphology of the Florida Peninsula.
White, W.B., 2007. Cave sediments and paleoclimate. Journal of Cave and Karst Studies 69, 76–93.
White, W.B., Vito, C., Scheetz, B.E., 2009. The mineralogy and trace element chemistry of black manganese oxide deposits from caves. Journal of Cave and Karst Studies 71, 136–143.
Wickert, A.D., Mitrovica, J.X., Williams, C., Anderson, R.S., 2013. Gradual demise of a thin Southern Laurentide ice sheet recorded by Mississippi drainage. Nature 502, 668–671.
Wright, E.E., Hine, A.C., Goodbred, S.L., Locker, S.D., 2005. The effect of sea-level and climate change on the development of a mixed siliciclastic-carbonate, deltaic coastline: Suwanee River, Florida, USA. Journal of Sedimentary Research 75, 621–635.
Wurster, C.M., Patterson, W.P., McFarlane, D.A., Wassenaar, L.I., Hobson, K.A., Beavan-Athfield, N., Bird, M.I., 2008. Stable carbon and hydrogen isotopes from bat guano in the Grand Canyon, USA, reveal Younger Dryas and 8.2 ka events. Geology 36, 683–686.
Yamamoto, N., Kitamura, A., Irino, T., Kase, T., Ohashi, S., 2010. Climatic and hydrologic variability in the East China Sea during the last 7000 years based on oxygen isotopic records of the submarine caverniculous micro-bivalve *Carditella iejimensis*. Global and Planetary Change 72, 131–140.